DESIGN OF A CENTRALIZED MICROGRID CONTROLLER IN COMPLIANCE WITH IEEE 2030.7 STANDARD

A THESIS SUBMITTED TO
THE GRADUATE SCHOOL OF NATURAL AND APPLIED SCIENCES
OF
MIDDLE EAST TECHNICAL UNIVERSITY

BY

SOHEIL POURALTAFI-KHELJAN

IN PARTIAL FULFILLMENT OF THE REQUIREMENTS
FOR
THE DEGREE OF MASTER OF SCIENCE
IN
ELECTRICAL-ELECTRONICS ENGINEERING

SEPTEMBER 2021

Approval of the thesis:

DESIGN OF A CENTRALIZED MICROGRID CONTROLLER IN COMPLIANCE WITH IEEE 2030.7 STANDARD

submitted by **SOHEIL POURALTAFI-KHELJAN** in partial fulfillment of the requirements for the degree of **Master of Science in Electrical-Electronics Engineering Department, Middle East Technical University** by,

Prof. Dr. Halil Kalıpçılar
Dean, Graduate School of **Natural and Applied Sciences** __________

Prof. Dr. İlkay Ulusoy
Head of Department, **Electrical-Electronics Engineering** __________

Assoc. Prof. Dr. Murat Göl
Supervisor, **Electrical–Electronics Engineering, METU** __________

Examining Committee Members:

Prof. Dr. Ali Nezih Güven
Electrical–Electronics Engineering, METU __________

Assoc. Prof. Dr. Murat Göl
Electrical–Electronics Engineering, METU __________

Assoc. Prof. Dr. Ozan Keysan
Electrical–Electronics Engineering, METU __________

Prof. Dr. Saffet Ayasun
Electrical–Electronic Engineering, Gazi University __________

Prof. Dr. Işık Çadırcı
Electrical and Electronics Engineering, Hacettepe University __________

Date: 10.09.2021

I hereby declare that all information in this document has been obtained and presented in accordance with academic rules and ethical conduct. I also declare that, as required by these rules and conduct, I have fully cited and referenced all material and results that are not original to this work.

Name, Surname: Soheil Pouraltafi-Kheljan

Signature :

ABSTRACT

DESIGN OF A CENTRALIZED MICROGRID CONTROLLER IN COMPLIANCE WITH IEEE 2030.7 STANDARD

Pouraltafi-Kheljan, Soheil
M.S., Department of Electrical-Electronics Engineering
Supervisor: Assoc. Prof. Dr. Murat Göl

September 2021, 94 pages

With the incorporation of renewable distributed energy resources and electric vehicles and battery storage systems into the conventional grid structure, the need for a microgrid and its control is emerging. IEEE 2030.7 Standard defines the Microgrid control system as a key element of microgrid regulating every aspect of it at the point-of-interconnection (POI) with the distribution system and autonomously manages operations such as transitions of operating modes. This system consists of control functions, which can be layered into the high, core, and low-level functions. The core-level functions comprise dispatch and transition functions, while the high-level functions include supervisory operations. In the proposed approach, a system is developed to achieve real-time monitoring and control of a microgrid through a microgrid central controller that ensures the proper operation of grid-connected and island modes. The microgrid system includes photovoltaic units, electric vehicles, battery storage systems, and bi-directional grid connections. A rule-based core-level dispatch function guarantees the security of supply to critical loads during the islanded mode. The core-level transition function accomplishes a successful transition between the operation mode. As a high-level function, the optimal operation of the microgrid in grid-connected mode is found by a model predictive control (MPC) based algorithm that incorporates the future reference information of the generation and load forecasts into the battery storage systems and vehicle to grid and vice versa control problem. Moreover, a communication framework and a graphical user interface are implemented.

Keywords: Microgrid, microgrid controller, electric vehicle, photovoltaic systems

ÖZ

IEEE 2030.7 STANDARDINA UYGUN BİR MERKEZİ MİKRO ŞEBEKE DENETLEYİCİ TASARIMI

Pouraltafi-Kheljan, Soheil
Yüksek Lisans, Elektrik ve Elektronik Mühendisliği Bölümü
Tez Yöneticisi: Doç. Dr. Murat Göl

Eylül 2021 , 94 sayfa

Yenilenebilir dağıtılmış enerji kaynaklarının ve elektrikli araçların ve pil depolama sistemlerinin geleneksel şebeke yapısına dahil edilmesiyle birlikte, bir mikro şebekeye ve kontrolüne olan ihtiyaç ortaya çıkmaktadır. IEEE 2030.7 Standardı, Mikro şebeke kontrol sistemini, dağıtım sistemi ile bağlantı noktasında (POI) her yönünü düzenleyen ve çalışma modlarının geçişleri gibi işlemleri özerk olarak yöneten mikro şebekenin kilit bir unsuru olarak tanımlar. Bu sistem, yüksek, çekirdek ve düşük seviyeli işlevlere katmanlanabilen kontrol işlevlerinden oluşur. Temel düzey işlevler, sevk ve geçiş işlevlerini içerirken, üst düzey işlevler denetim işlemlerini içerir. Önerilen yaklaşımda, şebeke bağlantılı ve ada modlarının düzgün çalışmasını sağlayan bir mikro şebeke merkezi kontrolör aracılığıyla bir mikro şebekenin gerçek zamanlı izlenmesini ve kontrolünü sağlamak için bir sistem geliştirilmiştir. Mikro şebeke sistemi, fotovoltaik üniteleri, elektrikli araçları, akü depolama sistemlerini ve çift yönlü şebeke bağlantılarını içerir. Kural tabanlı bir çekirdek düzeyinde sevk işlevi, adalı mod sırasında kritik yüklere tedarik güvenliğini garanti eder. Çekirdek seviye geçiş işlevi, çalışma modu arasında başarılı bir geçiş gerçekleştirir. Üst düzey bir işlev olarak, mikro şebekenin şebekeye bağlı modda optimum çalışması, üretimin gelecekteki referans bilgilerini ve yük tahminlerini akü depolama sistemlerine ve araca dahil eden bir model tahmine dayalı kontrol (MPC) tabanlı algoritma ile bulunur. Ayrıca, bir iletişim çerçevesi ve bir grafik kullanıcı arayüzü uygulanmaktadır.

Anahtar Kelimeler: Mikro şebeke, mikro şebeke kontrolörü, elektrikli araç, fotovoltaik sistemler

To My Beloved Family,

Alireza Pouraltafi-Kheljan

Leila Rotami-Kheljan

Kosar Pouraltafi-Kheljan

ACKNOWLEDGMENTS

I want to express my deepest gratitude to my supervisor, Assoc. Prof. Murat Göl for his support, guidance, advice, criticism, encouragement, and insight throughout the research. Prof. Gol has been a mentor for three years, and I am grateful for his support and wisdom.

I also would like to thank Assoc. Prof. Ozan Keysan, who co-supervised me in the ENERJİSA Project. It has been my honor and pleasure to work with him as a creative and supportive advisor. All the friends in the " Power System Analysis Laboratory" have taught and supported me from the first days at METU.

This research was funded by ENERJISA industrial project," Mikro Şebeke Kontrol ve Haberleşme Cihazı Geliştirilmesi Projesi," and the Scientific and Technological Research Council of Turkey (TUBITAK) under grant number 119E209. I want to thank Mr. Erdem M. Sezgin, Mr. Ozan Aktürk, and Mr. Mehmet Beyarslan, the other researchers of my participating project. It has been my pleasure to work with these ambitious researchers. Also, It was a great pleasure for me to cooperate with Mr. Mesut Uğur, Mr. Efecan Bozulu from Earsis Technologies.

I am grateful to my best friend Amirreza Azimi, whom I had his support and compassion. I made almost all of my critical decision with his consultant in these recent years. I hope we will keep this forever.

Lastly, I would like to thank my precious family and beloved girlfriend, Dr. Aysan Derakhshi-radvar, for their incredible support. They have always been more supportive and loving to me than I could ever imagine. I want to dedicate my degree to all their sacrifice.

TABLE OF CONTENTS

APPENDICES

LIST OF TABLES

TABLES

LIST OF FIGURES

FIGURES

LIST OF ABBREVIATIONS

CB	Circuit breaker
CL	Controllable loads
CCL	Continuously controled loads
DCL	Discretely controled loads
DG	Diesel generator
DER	Distributed energy resources
DES	Distributed energy storage
DL	Deep learning
DSO	Distribution system operator
EDO	Emergency dispatch order
EMS	Energy management system
GUI	Graphical user interface
G2V	Grid to vehicle
HVDC	Heat, ventilation, and air conditioning
LSTM	Long short-term memory
MCS	Monte Carlo simulations
MPPT	Maximum Power Point Tracking
MPC	Model predictive control
MG	MicroGrid
MCCD	Microgrid Control and communication device
MCMS	Microgrid controller multi-tread server
MGCS	MicroGrid control system
PMPVG	Possible maximum PV generation
POI	Point-of-interconnection

RNNs	Recurrent neural networks
SMPC	Stochastic model predictive control
SS1	Grid-connected mode
SS2	Islanded mode
T1	Unplanned islanding
T2	planned islanding
TCP	Transmission control protocol
V2G	Vehicle to grid

CHAPTER 1

INTRODUCTION

The 2003 Northeast Blackout was one of North America's most significant power outages, making it suitable for research and lessons gained [1]. Based on the several studies, [1, 2, 3, 4], causes of this event can be summarized as the inadequacy of system understanding, reliability coordinator diagnostic support, situational awareness, and tree trimming. The generally proposed solution to overcome these problems is smart grid and microgrid (MG) concepts that better utilize existing sources.

Microgrids have a long and illustrious history. The first power plant constructed by Thomas Edison, the Manhattan Pearl Street Station, built in 1882, was effectively a microgrid [5]. Also, integrating microgrids (MG) is expected to solve most of the technical problems caused by the integration of DERs. As a result, the necessity for central coordination will reduce, and the realization of the smart grid will be more straightforward.

There is no unique definition for MGs, and all present definitions are quite similar, with only minor differences. MG's most commonly recognized factors are the control framework for generation and demand, well-defined limits, and islanding capabilities [6, 7, 8, 9]. Microgrids are primarily electrical, including AC, DC, or hybrid systems, but they can also include thermal components for heating. Because the difference of load generation points is small, the system's norms are less than the main network. Microgrids enable the combined operation of distributed energy resources (DERs) and energy storage systems considering system reliability [10, 11]. According to [6], MGs can be defined as distributed power systems, which can operate either in grid-connected mode or island mode. According to [12], a microgrid should have the following capabilities:

1. It should operate both in grid-connected mode and in isolated mode,
2. It should allow transitions between modes of operation,
3. In grid-connected mode, it can sell the excess power or ancillary services,
4. In island mode, it should operate as a grid forming system.

To rationalize the installation of a microgrid, one must first determine its influences (the results of the microgrid's development and operation), payoffs (the costs and advantages of its implementation and management), and stakeholders (who will be affected by the microgrid). Microgrids can provide relevant parties with a range of socio-economic, technical benefits and impacts. It is useful to differentiate between the concepts of "impacts" and "benefits."

The numerous changes that arise from installing and operating a microgrid in various systems are called "impacts." Impacts might range from extremely technical and clearly verifiable to vague instances [13]. Authors of [8] divide microgrid impacts into two : "known impacts" (those that must be recognized as time passes by) and "discovered impacts" (those that must be discovered by simulation or computation of particular input data).

In contrast, "benefits" are described as the actual financial advantages that stakeholders gain from a microgrid. Although certain impacts may have direct economic value, non-economic microgrid impacts must be mapped onto obvious economic advantages to stakeholders to establish a business case. It should be noted that "costs" might merely be defined as negative benefits [8]. Microgrids' direct, significant technical and economic benefits have been summarized as lower cost and more profit [14], higher efficiency, lower emissions, and ameliorated power quality [15] and reliability [16] .The indirect advantages of microgrid operation are more diverse, but they are also harder to define. This set includes environmental advantages such as reducing the necessary physical track required for electricity generation, and reducing dependency on fossil fuels [17].

Although microgrids are presented as next-generation power system structures, they have some issues about their operation:

- Bi-directional power flows
- Stability problems during transitions
- System modeling
- Low inertia
- Uncertainty

Standards contribute to the advancement of microgrid installation and configuration by having a comprehensive technical basis for interconnection and interaction with the utility grid at the point of interconnection. Standardization of MG controllers is necessary to offer [18]:

1. A common technical base for defining controller functions
2. A reference point and interpretation to policymakers and authorities for the microgrid's operating capabilities

There are six main standards related to MGs [19]. The IEEE 1547.4 standard [20] provides a reference for the design, operation, and transition of DER, such as the transition to island mode, island mode operation, or the reconnection mode, which can be referred to as a microgrid. A new version of this standard, IEEE 1547-2018 [21] was published in 2018. IEEE 2030.7 standard [9] addresses the functions higher than the component control level related to the appropriate operation of the microgrid energy management system common to all microgrids, disregarding the application, topology, configuration, or administration. In this standard, Control functions can be levelized into the high, core, and low levels. The detailed description of this document is presented in the following section. IEEE 2030.7 standard cites IEEE 2030.8 [22] standard to qualify, verify and evaluate the recommended specifications and functionalities. As a result of these tests, microgrid controllers may be adopted more broadly. IEC 62898 series includes IEC 62898-1 [23] and IEC 62898-2 [24]. IEC 62898-1 covers the technical requirements and guildlines for the microgrid planning stage. IEC 62898-1 intends to provide principles and requirements related to components, operation, and transitions.

1.1 Microgrid Components

The main characteristic of MGs which differentiates them from virtual power plants (VPP) is their structures. Distributed energy resources (including small conventional units and renewables), energy storage, various loads, and conventional power plants are typically included in VPPs, and VPPs are mingled by the utility grids. However, MGs are connected from a single point to the utility grid. Therefore they can operate in both grid-connected and islanded mode [5]. In Figure 1.1, the possible units of a microgrid are illustrated. Generally, components of the MG can be classified into five sets [9]:

1. Components connecting the microgrid to the utility grid at the point-of-interconnection (POI) such as disconnectors and circuit breakers
2. Microgrid control system (MGCS)
3. Local distribution system components such as transformers, switch-gears, capacitors
4. Breakers or dis-connectors for internal interaction and interconnection of MG elements
5. Physical devices: DERs, controllable loads, distributed energy storage (DES), and loads

IEEE 2030.7 standard categorizes microgrid loads into different types in terms of their critically and controllability:

1. *Critical loads*: These are loads that must be supplied in all of the microgrid's regular operation conditions. They are generally are not controlled. Building controls, security systems, life-safety systems, information technology servers are instances of this set.
2. *Priority loads*: These are loads that can be regularly disturbed or adjusted at different load levels. Lighting, elevators, HVAC system loads (chillers, air - conditioning units), and non-essential industrial process equipment are examples

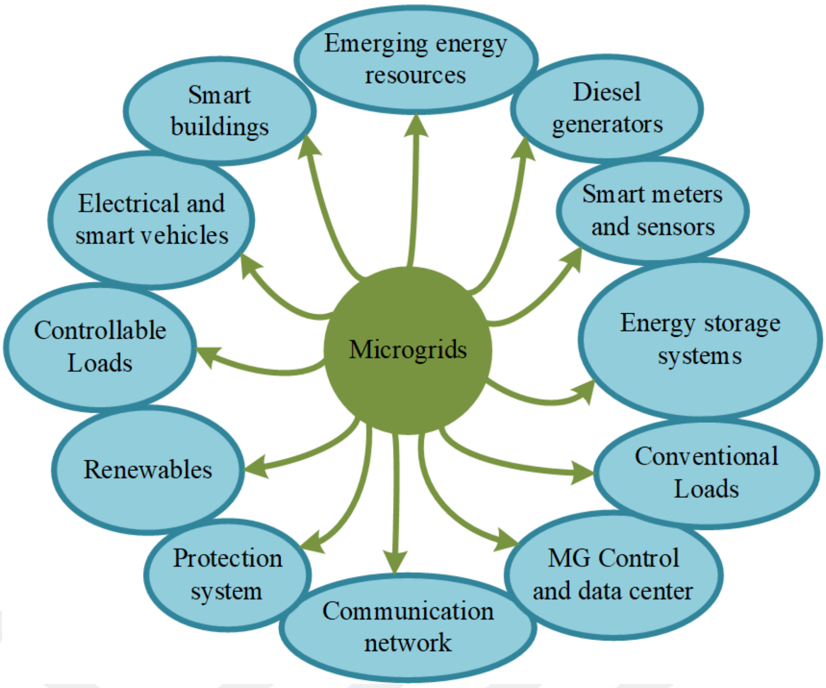

Figure 1.1: Microgrid units

of this set. Building HVAC systems can have their operating points modified to offer regulated loading.

3. *Interruptible loads*: These are loads that can be shed or interrupted at any time to balance generation and demand. Examples include thermal energy storage, water pumping where enough tank storage is available, and charging of batteries in DES devices.

4. *Diversion and dump loads*: These loads are used when excess generating capacity is available, and curtailment of generation is either not possible or where there is an economic benefit using the diverted energy. An example is a diversion load for a wind turbine that absorbs gust energy.

5. *Undefined loads*: loads with unclear behavior that are not included above.

Based on the operating conditions of the MG, different load categories are connected to or disconnected from the MG to maintain the generation and load balance, and MG stability. These actions are accomplished through a circuit breaker controller and controllable load's local control.

The breaker controller monitors and initiates the MG breakers. The implementation method depends on the available breaker and its compatibility. The breaker controller receives the breaker control signal from the microgrid control system and sends a breaker status and manually by operators. Breaker status includes one of these modes, including open, closed, and tripped.

Microgrids may involve various kinds of DERs. Those might be renewable energy resources such as photovoltaic (PV) systems, wind turbines, microturbines using CHP systems, and fuel cells or conventional generators. Local controllers of the DER and DES devices maintain the required frequency and voltage. However, control modes and set points of these assets are assigned by the microgrid controller. In microgrid islanded mode, at least one of these devices should provide the grid forming.

Basically, DERs can be divided into two categories in terms of connection types to the distribution system. These are conventional synchronous machines directly connected to the distribution system and renewable resources connected to the distribution system with an electronic converter [25]. The control strategies of these two types of DERs are entirely different from each other. DERs can also be grouped in terms of their dispatch characteristics. Non-dispatchable DERs are generally working at the optimum operating point. Especially in renewable energy units, the Maximum Power Point Tracking (MPPT) system is used due to the intermittent character of the renewable energy sources. In this way, always the maximum possible power is drawn from the energy source. However, with this control method, the produced power depends on the current state of the energy source and prevents economic dispatch. It is possible to use these distributed power generation units and energy storage systems to make economic dispatch possible [26]. In Figure,1.2 both a non-dispatchable PV system and a dispatchable PV and BSS combination are represented. IEEE Standard 1547 provides detailed information about multiple DERs interconnection to power grids [20].

Following DERs can be considered in MG's structure, but it is not limited to these mentioned resources:

1. Dispatchable

- Diesel generators
- Combined Heat and Power (CHP)

2. None-dispatchable

- Wind turbines
- Photovoltaic arrays/ inverters

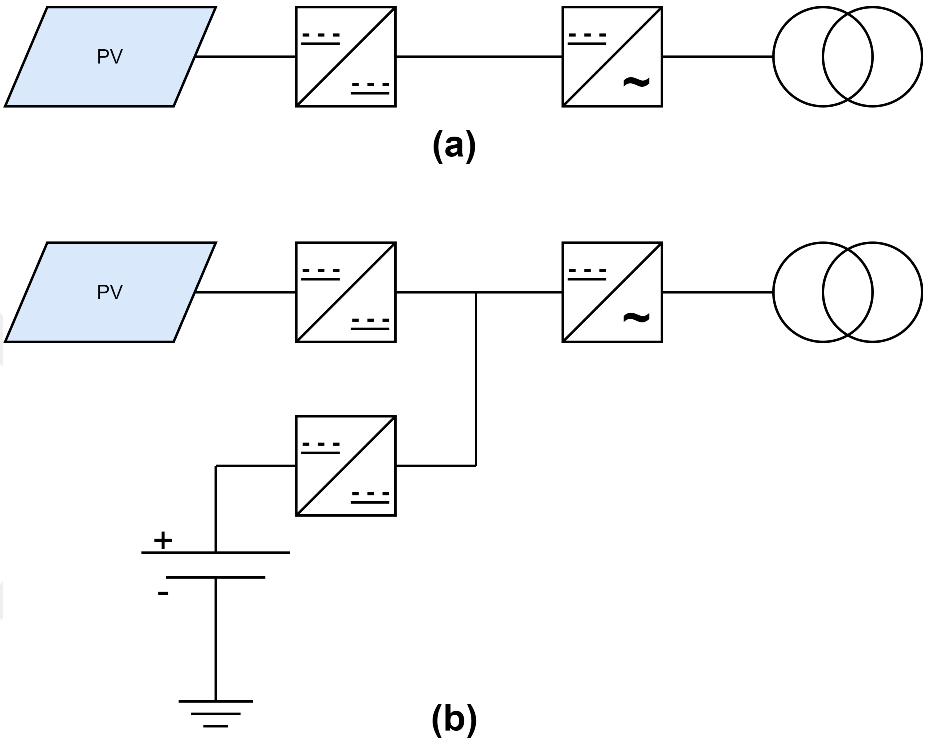

Figure 1.2: Two possible configurations for the PV system: (a) A non-dispatchable PV unit. (b) PV unit and energy storage system integration becomes dispatchable

DERs local controller accepts the following commands from the MGC:

1. Control mode commands: grid forming (isochronous, droop), grid supporting, and grid feeding,
2. Real power setpoint ,
3. Reactive power setpoint ,
4. Voltage setpoint,
5. Start or stop.

In case of having enough communication and monitoring infrastructure, the local controller provides the following real-time values for MGCS:

1. Real power output, reactive power output, power factor output,
2. Power quality (harmonic distortion),
3. Local bus voltage, current,
4. Generation capability curves (current maximum and minimum available P, Q of the unit), percent loading, fuel utilization, fuel remaining,
5. Device ratings and self-describing information.

The primary application of the DES is to coordinate with DGs to enable microgrid generation adequacy. DES also has a local controller system and operates in cooperation with the MGC. For this purpose, MGC determines the following setpoints for this local controller:

1. Control mode: Grid forming (isochronous, droop), grid supporting, grid feeding,
2. Real Power output setpoint, reactive power output setpoint,
3. Real Power input setpoint, reactive power input setpoint.

Also, DES provides the following real-time values for the MGC:

1. Voltage, current,
2. Storage capacity(kWh) (current, maximum) and Power output maximum,
3. State of charge.

Moreover, an electric vehicle's available storage can play an important role following the DES system. This participation can be accomplished in both directions so that the vehicle's battery can be charged from the grid (G2V). In the necessary time, the vehicle's battery can be considered an energy resource. Energy is derived from the vehicle to the grid (V2G). Following related values presented to the MGC:

1. Number of plugged-in cars,
2. Divers' permission for V2G action,
3. Available vehicle storage capacity,
4. The available usable stored energy of vehicles.

While developing a microgrid controller, the aforementioned issues should be taken into account. The developed controller should have the following main specifications:

- Output control of DERs in terms of voltage and frequency,
- Power balance in microgrid,
- Demand-side management,
- Economic dispatch,
- Transition between operating modes of a microgrid. Especially seamless transition to island mode is very crucial [27].

1.2 Literature Review of Microgrid Control System

Control and operation in a microgrid are critical factors in the success of electrical systems due to numerous restrictions, such as control functionality in islanded operation or power exchange with the main grid. This topic has a large amount of scientific and industrial literature. This system layer may be composed of only the software or both software and hardware. In microgrid control, a hierarchical control method should be followed [12, 28, 29, 30, 31, 32, 33]. In Figure 1.3, the microgrid control scheme is given. It should be noted that tertiary control is not an applicable approach for such small-scale grid structures.

While the main grid controls the voltage magnitude and frequency, the main control parameters are the active and reactive power output of the DERs in grid-connected mode. However, in island mode, there is no reference voltage for DERs, so this mode is quite challenging. Even short duration of voltage and frequency inconsistency may

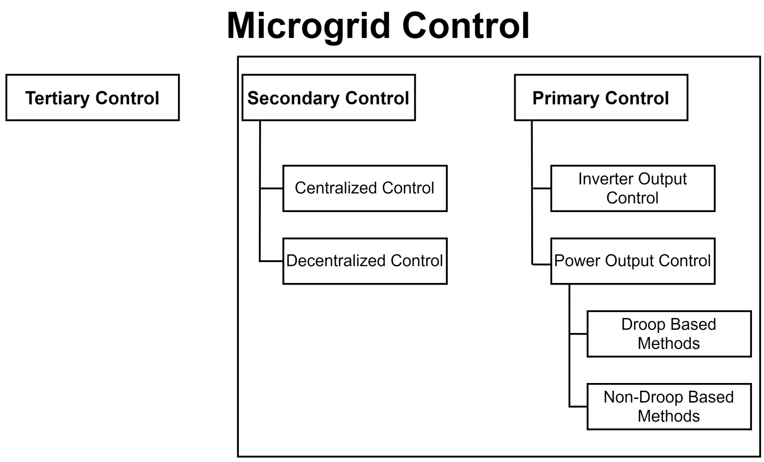

Figure 1.3: Microgrid control methods

result in large current circulations [30, 29]. An intuitive method is given in [33], where a DER is set to produce system voltage, frequency, and other units that provide the power balance in the microgrid.

Primary control is the fastest control mechanism, thanks to its local measurements and communication-free approach. Therefore, control of unit connection status, output voltage control, and output power balance control is achieved with this control method [12], [27]. Although the most popular methods for primary control are droop based methods, they have some disadvantages [34]:

- Bad transient response, due to the use of rated powers,
- Performance problems due to the omission of load dynamics,
- High coupling between active and reactive power due to low X/R ratio,
- Stability issues due to load harmonics.

In literature, some works are defined to overcome these issues [31], [32].

Secondary control is a more sophisticated control step. Changes in voltage magnitude and frequency are corrected in this step. Two main controller approaches are given in the literature, namely centralized and decentralized control methods. Some basic advantages and disadvantages of those methods can be seen in Table1.1 [35, 36, 37, 38]. Implementation of decentralized controller techniques requires more advanced tools; therefore, in this study, centralized controllers will be the main focus.

Table 1.1: Advantages and disadvantages of secondary control methods

Type	Advantages	Disadvantages
Centralized Control	Simpler control algorithms	Communication burden
Decentralized Control	Low communication requirements	Cannot guarantee optimum operational point

According to [30, 37, 38], a centralized controller can be shaped with one of the following functions:

- Optimum economic dispatch,
- Bidding,
- Non-model based approaches,
- Inclusion of energy storage systems,
- Model-based approaches.

In centralized controllers, various methodologies can be used, like optimal dispatch, bidding method, etc.

Most of the existing microgrid control test benches focus on one specific function, and the tests are conducted without regard to a recognized standard. The microgrid energy management system coordinates the active and reactive power dispatch setpoints for the inter-dispatch intervals with the local primary power control loops used by the DERs [10]. Authors in [39] validate an MGCS with a dispatch function on a real-time testbed, but offline optimization is still performed. Similarly, the Authors of [40] present dispatch and protection functions, but no complete tests are undertaken. For grid-connected and islanded operation modes, S. Manson et al. propose [40] a control technique that uses an energy storage system (ESS) for power smoothing, keeping the state of charge (SoC) around 50%. Although the SoC can be tightly regulated, it is relatively conservative because the capabilities of ESS as an energy buffer for peak shaving and valley filling are not fully explored. In [41], a comparison of load-following control and cycle-charging control is performed on an islanded PV-diesel-ESS microgrid, where the ESS and diesel generator are used as the primary sources to achieve power balance. It has been discovered that using ESS to track load change might minimize fuel usage, although the energy stored in the system may be depleted sooner than expected [42]. The lifespan of ESS will be shortened by using a traditional cycle-charging approach with repeated deep discharges. Bo Zhao et al. [43] describe a hybrid adaptive rule-based dispatch for a realistic stand-alone microgrid that uses a diesel generator and energy storage to address power shortfall in several SoC ranges. The control approach, on the other hand, is still unable to achieve its objectives. Chu Sun et al. [44] developed a hybrid rule-based dispatch strategy as a microgrid central controller. The method keeps the BSS SOC around 0.5 for the sake of MG resiliency and reliability and to extend the BSS lifetime. Moreover, a dispatchable diesel generator (DG) is kept ON during the operating modes of the MG. Three control modes for the dispatch strategy are allocated based on overlapped SOC ranges.

More advanced control methods are drawing attention, and the so-called Model Predictive Control (MPC) method, which utilizes the model's forecast in each decision time, is one of them. There are works in the literature using MPC from simple approaches [45] to comprehensive ones [46, 47, 48, 49, 50]. In [45] authors use MPC to alleviate the thermal overloading in transmission lines. In [46] a successful implementation of MPC for a microgrid is given. Although renewable modeling is explicitly given in this work, the main principles of MPC are explained in detail. In [47] MPC, the application for the microgrid is explained, and the controller is tested in different market structures. In [48] authors use a two-stage stochastic programming approach to overcome uncertainties in load demand. From the objective function point of view, all of these works aim to minimize the cost of the operation. In [51], in addition to the operation cost, the aging of BSS and EV batteries is also added to the cost function. With the introduction of the aging effects, switching decisions of the batteries are smoothed. The employment of V2G systems addresses new business models with new participants supporting service to vehicles, buying or selling electrical energy, and cooperating with utility grids. Electrical Vehicles (EVs) participate in the microgrid central control strategies with various objects. Li et al. [52] presented an EV-based MPC algorithm to regulate the voltage. Frequency stabilization is maintained through MPC-based control of the microgrids with EV participation in

[53] and [54], while MPC is utilized to manage the charging of parked EVs and BSS to achieve the optimized economical solution in [55].

1.2.1 Review of IEEE 2030.7 Standard

IEEE-SA Board provides IEEE Standard for the specification of microgrid controllers (IEEE 2030.7™) [9]. The scope of this standard is to address the functions above the component control level associated with the proper operation of the Microgrid Energy Management System that is common to all microgrids, regardless of topology, configuration, or jurisdiction. There is a single limitation on microgrid topology: the microgrid shall connect to the distribution grid at the POI. The standard declared three distinct characteristics for any system to be considered as a microgrid:

1. Clearly defined electrical boundaries,
2. A control system to manage and dispatch resources as a single controllable entity,
3. Installed generation capacity that exceeds the critical load.

The MGCS includes the control functions that define the microgrid as a system that can manage itself, operate autonomously or grid-connected, and seamlessly connect to and disconnect from the main distribution grid to exchange power. It satisfies the interconnection requirements using functions at the high level, core level, or low level of its function stack given in Figure1.4. The lower level or device is related control action is performed via network components local control.

The main goal of building the core function is providing a framework to have a modular design of the microgrid control system employing the platform-independent interfaces. This standard defines functions and their interrelationships that allow modularity and interoperability in physical implementations. It deals with the operation of the microgrid control system and defines those aspects that need to be standardized; others can remain proprietary. In addition, the relationship and interaction between the dispatch and transition functions and control levels are illustrated in Figure1.5.

1. The dispatch function: dispatches individual devices in given operating modes and with specified setpoints
2. The transition function: supervises the transitions between connected and disconnected states and ensures the dispatch is appropriate for the given state.

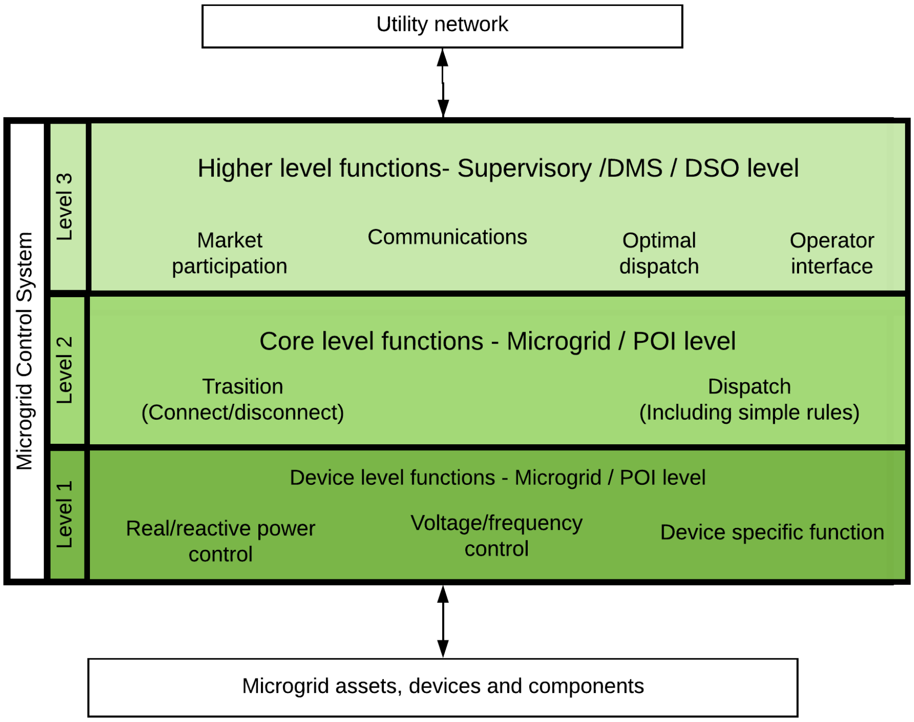

Figure 1.4: Microgrid control system functional framework. [9]

The dispatch function computes its dispatch order from a dispatch rule. In the simplest case, this rule is static and set up by the operator in the beginning. A value-added dispatch optimizer engine would be considered a higher-level function and optimizes dispatch by editing the dispatch rule in real-time. This modularizes the optimizer and dispatch functions, making modifications and upgrades of the optimizer easier.
The dispatch function coordinates microgrid assets for optimal and stable operation during each of six possible dispatch operating modes:

1. SS1 - grid-connected steady state,
2. SS2 - islanded steady state,
3. T1 - unplanned islanding,

4. T2 - planned islanding,

5. T3 – reconnection,

6. T4 - black start.

The dispatch function includes the dispatching of microgrid assets and providing them with appropriate setpoints. It directs the use of the distributed energy resources available within the microgrid. It ensures the proper operation of the microgrid, both internal to the microgrid and as seen by the grid at the POI with the distribution system. The dispatch function operates on a longer time frame than the transition function of the microgrid, typically in the range of minutes, compared to the range of milliseconds for the transition function. A dispatch order is a set of commands sent to the microgrid assets or their controllers from the dispatch function. The dispatch core function provides the following functionalities:

1. Balancing generation and load under normal islanded operating conditions,

2. Re-dispatching controllable resources in response to internal events related to the load and generation profiles.

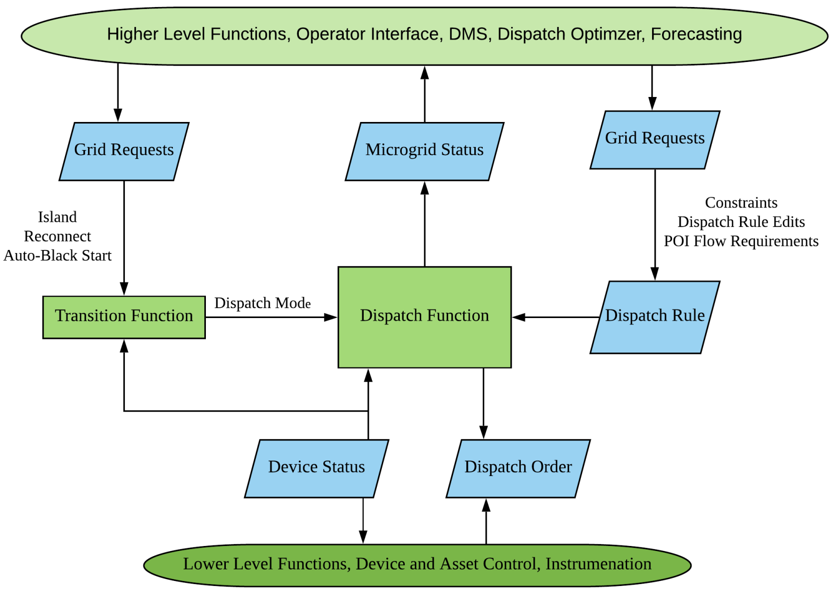

Figure 1.5: Relationship between transition and dispatch functions. [9]

To perform its functions, the dispatch function also receives microgrid system state information, and if necessary, estimates state information not directly observable. The exception to the above process is in the immediate execution of an emergency dispatch order (EDO) upon being set to unplanned island dispatch mode by the transition function. This dispatch order may include changes in generation dispatch and load shedding as required to match available generation to emergency loads. This order is continuously updated as conditions change and are available for execution without waiting to be computed.

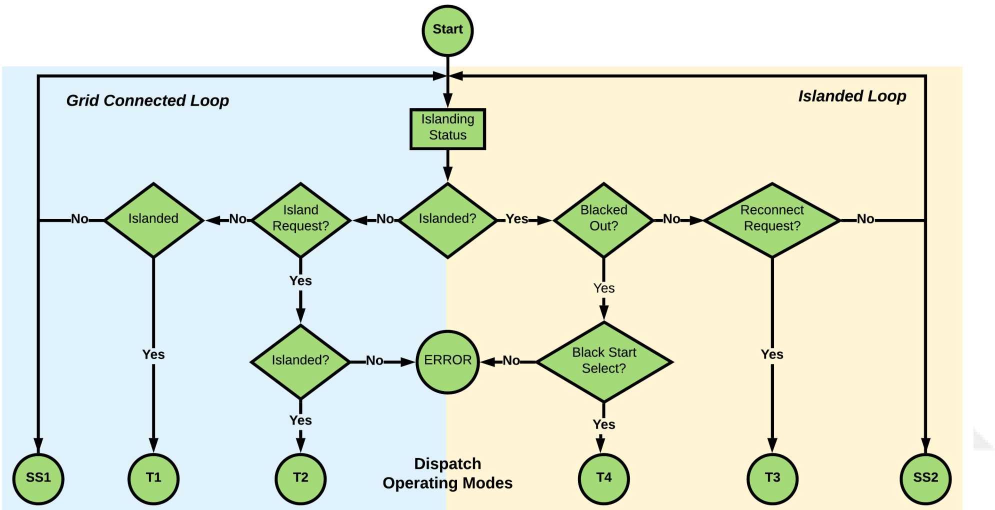

Figure 1.6: Sequences associated with the transition function. [9]

The logic of the transition function controls the mode in which the dispatch function in the MGC operates. The dispatch function accesses and implements the dispatch rules for each of these dispatch modes. The transition function is a rule-based algorithm to achieve all transitions, including seamless planned transition and unplanned transition into the islanded mode. The transition function executes the logic presented in Figure 1.6and sets the dispatch operating mode of the dispatch function. The transition function thus runs in one of two loops, connected state or islanded state. It sets the dispatch function to operate in the appropriate steady-state dispatch operating mode for the state of the microgrid. Upon detecting a transition event, it changes the dispatch operating mode of the dispatch function [9].

1.3 Contributions

In this thesis, the real-time monitoring and control action will be performed through the centralized microgrid control system alongside with an advanced field unit. This system is established by a central multi-thread server (CMTS). CMTS's interface with the MG components is a communication and control device (MCCD). MCCD is considered as a black box, and its internal functionalities are not addressed. The CMTS process the received data through the novel control functions and executes the required commands. These control functions are higher and core level functions in compliance with IEEE 2030.7 standard [9]. In the proposed MGCS, CMTS communicates with MCCDs located in the field through the TCP/IP sockets. Also, a graphical user interface (GUI) is provided for interaction with the microgrid operator. The operator can apply the required operation through this interface. Also, interconnection requirements can be received from the distribution system operator via a communication module. The interaction between components of the proposed MGCS and MCCD and corresponding data flow is illustrated in Figure 1.7.

Core-level functions include dispatch and transition. The generic dispatch function is designed based on a SOC-following dispatch rules and load management strategy. The load management strategy sheds and restores the determined amount of load regarding the critical and controllability of loads. It should be noted that there are load management approaches in other studies; however, those are not in compliance with specifications of IEEE standards for core-level functions. These control functions make the proposed MGCS flexible for different microgrids regardless of a microgrid's size and application. The transition function provides the logic to detect and perform proper transitions. The planned and unplanned islanding transitions are considered in this function.

On the other hand, as a higher-level function, stochastic model predictive control (SMPC) is an optimization-based control approach that minimizes the proposed cost function regarding the system's model and corresponding constraints within a specific time horizon. To achieve optimal dispatch, MPC incorporates future reference information based on the generation and load forecasts into the battery storage systems (BSS) and vehicle to grid (V2G) control problem. SMPC will be used for the cost optimization of the microgrid energy management system. Because this approach provides a methodological arrangement between feasible control action and the probability of state constraint violations in a stochastic framework [56]. Stochasticity will be added by using Monte Carlo Simulations (MCS) for both PV; since this approach does not use any mathematically complicated models and still gives satisfactory results. For the PV generation, both the stochastic approach with MCS and the deterministic prediction approach with long short-term memory (LSTM) will be presented. It should be noted that also a rule-based dispatch approach for SS1 dispatch is presented in the core-level dispatch function. These two functions will cooperate in a multi-layer framework with different time horizons.

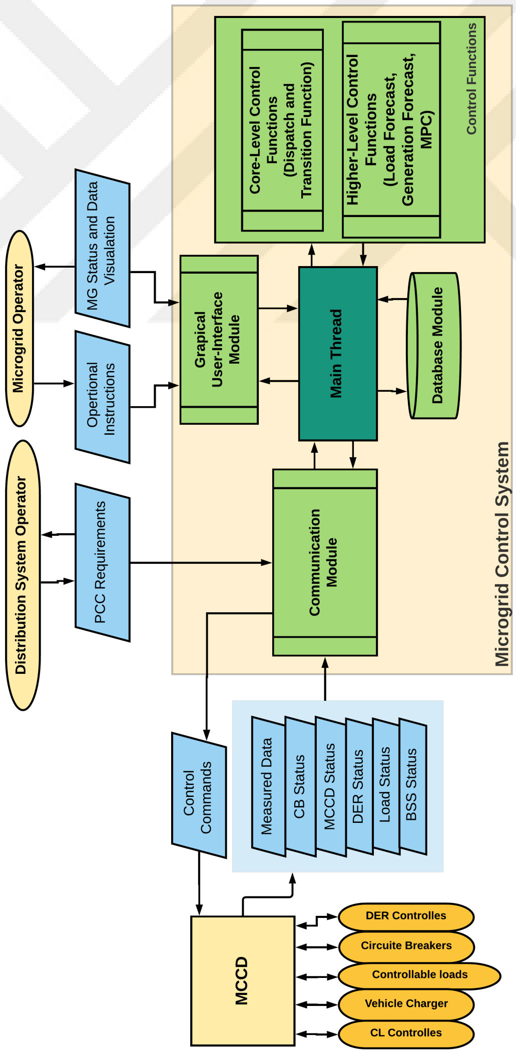

Figure 1.7: Data flow within the MGCS and MCCD.

The main objectives of this thesis are as follows:

1. To perform higher-level control functions over the MG to optimize the MG's energy cost during grid-connected steady-state (SS1), assuming the presence of PV units, EVs, BSS, and bi-directional grid connection,,
2. To provide reliable operation for the prioritized (critical) loads rather than the economic operation of the MG during island steady-state (SS2) by MGCC,
3. To perform successful transition modes, including unplanned islanding (T1), planned islanding (T2),
4. To implement a proper communication framework between the CMTS and MCCD,
5. To provide a graphical user interface for data visualization and manual control for MG operator.

1.4 Thesis Outline

In this thesis, the work is presented in six chapters. The structure of the thesis is given as follows:

The first chapter is the introduction where the motivation for microgrid and microgrid controllers is given, and the scope of this thesis is explained. Moreover, the literature review of the related works is given, and contributions and objectives of this study are itemized.

The proposed MGCS is presented in the second chapter, and related components and their interactions are introduced. The necessity of a multi-thread server for this MGCS and related implementation is presented. Also, compliance of centralized controller with IEEE 2030.7 standard is explored, Database, communications, and graphical user interface modules are explained in detail.

In the third chapter, core-level functions are the proposed MGCS are given. This layer of functions includes dispatch and transition functions. The dispatch consists of different rules, emergency dispatch order, and load management strategy are described in related sub-sections,

The fourth chapter is related to the higher-level function of the proposed MGCS. This set includes two different modelings for PV generation forecasts alongside MPC and SPMC optimal dispatch approaches. In SMPC, the stochasticity of PV generation is handled using Monte Carlo simulations. Also, MPC utilizes the LSTM for PV forecast modeling. These functions are proposed to manage BSS, G2V, and V2G operation considering economic optimality.

The simulation test results of the proposed control function are given and discussed.

In conclusion, which is the sixth chapter, the aim and success of this work are given. Also, future work to improve the control and monitoring performance of MGCS is explained.

Finally, tabs and sub-tabs of the proposed graphical user interface are illustrated in Appendix A.

CHAPTER 2

THE CENTRALIZED MICROGRID CONTROL SYSTEM

The previous chapter presents the main impetuses of microgrids and the benefits of a centralized microgrid controller. The necessity of standardization for MGCSs and a summary of the related document are discussed. Also, the related literature survey to the centralized microgrid controllers was explored. In this chapter, a centralized microgrid controller will be proposed. This system is composed of hardware and software parts. The software part is a multi-thread central server, which is the main contribution of this thesis. Different components of this server will be given in the following subsections.

The ubiquitousness of real-time monitoring and command and control across the nodes of the system differentiates a smart microgrid from a conventional system. That requires relevant microgrid nodes to have the capability of generating real-time data and communicating those with other nodes across the system regardless of where these nodes are or what their functions may be. In other words, monitoring and control within a smart microgrid system must be an end-to-end exercise and encompassing (preferably) all network nodes. That requirement calls for command and control strategies capable of dealing with microgrid events through localized intelligence. Be-sides, individual components, such as energy converters, batteries, etc., may have dedicated management and control intelligence, interfacing with higher-level control systems and applications to receive set-points and inform them of their status and events. Accordingly, MGCS is a centralized system that is consisted of control functions defining the microgrid as a single entity that can act separately.

The MGCS obtains the required information, including frequency, voltage, and current phasors, active, reactive, and apparent power, circuit breaker (CB) status, MCCD status, and controlled device status from MCCDs. MCCDs are not the single information source for MGCS. The distribution system operator (DSO) and MG operator (MGO) can also send the MGCS. On the other hand, commands executed by the control function to manage the microgrid and commands provided MCMS and user interface are transmitted from MCMS to MCCD applying to MG assets.

The main components of the proposed MGCS illustrated in Figure 2.1 are as following:

1. Communication module,
2. Database module,
3. Graphical user-interface,
4. Core-level functions,
5. Higher-level functions.

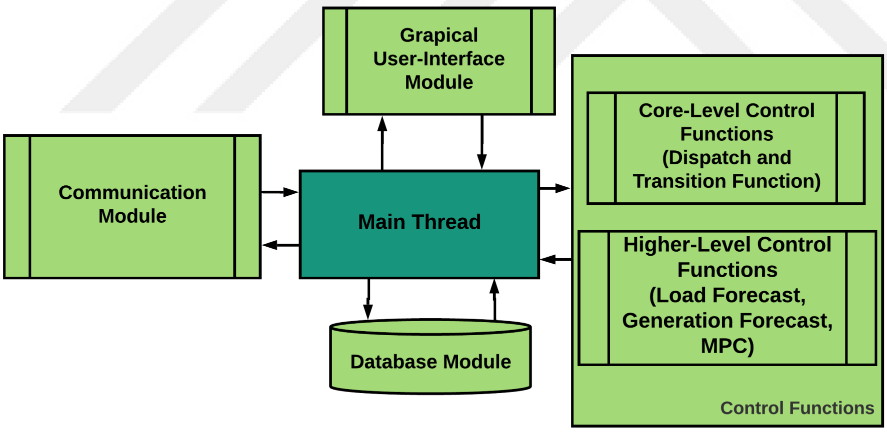

Figure 2.1: Components of the MGCS.

All components of MGCS are required to operate concurrently, and the corresponding computation of none of them can be interrupted by other tasks. In such conditions, the utilization of multiple threads is one of the wieldiest solutions. With the help of threads, different operations can be executed simultaneously. It should be noted that threads may not be running on different processors at the same time. Some threads may run on the same processor. As a result, in terms of computation time, it may not be the most efficient solution. However, they do allow for the operation of multiple code parts at the same time [57]. Accordingly, each module of central server software is executed in a separate thread.

Details related to the database, communication, and GUI modules are presented in the following subsections. Core-level and higher-level functions are explained in chapter 3 and chapter 4, respectively. Also, an operation classification is fulfilled and presented.

2.1 Operator Control

Operators control the microgrid by providing inputs to the transition function and the dispatch rule. Those inputs are as follows:

1. Inputs to the transition Function:
    - Planned Island Request.
2. Inputs to the dispatch Rule:
    - Constraint steady-state connected dispatch to ensure successful unplanned islanding.
        - Constrain the dispatch of any physical asset,
        - Physical constraints of the system (such as generator ramp rates),
        - Fuel availability.
    - Dispatch rule edits to change the priorities and logic of the dispatch rules for any of the dispatch modes. An example is the scheduled maintenance of the generating units.

Moreover, some of the operations in MG are performed manually by operators. This action is mostly related to the maintenance issues of the MG. Automatic and manual operations in the MG are presented in Table 2.1.

Table 2.1: MG operations' classification

Operation	Automatic	Manual
Planned islanding	Yes	Yes
Unplanned islanding	Yes	Yes
Black start	Yes	No
Switch to connected mode	Yes	Yes
Voltage control	Locally by means of the device-level control and determination of DERs' operating mode by MGCS	No
DES control	Yes	In case of maintenance
Diesel generator islanding	Due to the dispatch order of MGCS or locally in case of the presence of disturbances in MG	In case of maintenance
DER islanding	Due to the dispatch order of MGCS or locally in case of the presence of disturbances in MG	In case of maintenance

2.2 Communication Module

Real-time communication between the MCCD and the CMTS takes place over the Internet network. The internet transmission control protocol (TCP) is used to enable end-to-end data communication over the Internet. It specifies all the necessary processes, such as how data should be packaged, addressed, transmitted, forwarded, and received. TCP is used to define how applications create channels to communicate over a network. TCP also allows the arrangement of packet size for messages before they are transmitted. IP is used to address and route individual packets so that they reach the correct destination. Thanks to TCP/IP, data loss is prevented during end-to-end communication, although this functionality may cause some time delays [58]. Therefore, a suitable method for data acquisition should be used in the implementation.

The exchange of data among the different components of MGCS is the main common interface of these components. These messages and corresponding transmission

Table 2.2: Description of messages transmitted between CMTS and MCCD.

Message's name	Send frequency
From MCCD to MCMS	
IDBIT result report	As requested by CMTS
ODBIT result report	After the connection is established or as requested by CMTS
Administrative Status	As requested by CMTS
Digital administration response	In response to switching command
Analog administration response	In response to the analog set command
Location Information	As requested by CMTS
Maintenance mode status	As MCCD is taken to maintenance mode
Phasor measurements report	10 Hz
Other measurements report	10 Hz
From MCMS to MCCD	
ODBIT inquiry	After the connection is established to assign ID for the MCCD
Administrative status inquiry	As the switches' status and analog setpoints in the system is queried
Numerical administration instruction	As the switches' the status will be set
Analog administration instruction	As the analog setpoints will be set
Location information inquiry	As requested by CMTS

frequency are given in Table 2.2, where IDBIT and ODBIT stand for initialization device-built-in and operational device-built-in tests, respectively. These messages include the status and related information of modules of MCCD. All the data packages transmitted include Sender, receiver, and the data type of message, message, and message ID.

In Table 2.2 the phasor measurements report include:

- Three-phase voltage magnitude for three channels,
- Three-phase voltage angle for three channels,
- Frequency for three channels,

- Three-phase + neutral, current magnitude for three channels,
- Three-phase+ neutral, current angle for three channels,
- Timestamp.

The other measurements report include:

- Three-phase voltage RMS values for three channels,
- Three-phase + neuter, current RMS values for three channels,
- Total apparent power values for each of three channels,
- Total active power values for each of three channels,
- Total reactive power values for each of three channels,
- Three-phase power factor values for three channels.

2.3 Database Module

It seems necessary for the MGCS to have a database to store the events, executed commands, and measured and processed data for future applications. The stored data is accessed and exported through the user interface. The related time scheduling and strategy for this data storage are critical due to the storage limitation, and technical considerations. The data update resolution and storage duration are illustrated in Table 2.3.

2.4 Graphical User Interface Module

Real-time monitoring and manual control are the main purposes for the implementation of the User-Interface. The UI should provide the opportunity to make the microgrid operator able to explore the historical data related to the MGCS. Moreover, the operator should be able to observe the corresponding forecasts to renewable generation and load. Python environment is utilized to implement the proposed UI. For

Table 2.3: The storage strategy in the database module.

Data	Resolution	Storage duration
Three-phase voltage and current phasor and RMS measurements, frequency, active power, reactive power, apparent power, and power factors	10 Hz	24 hours
	1-second average	One day
	1-minute average	One month
	5-minutes average	One year
	1-hour average	Ten years
Forecasts	15 minutes	One year
	1-hour average	Ten years
Executed commands	-	One year
MCCD status error reports	-	Six months
MGCS error reports	-	Forever
Calendar	Once a year	One year
Academic calendar	Once a year	One year
Weather	Once a minute	One year
Network topology and parameters	In case of change	Forever

this purpose, several Python libraries are utilized, including "PyQt5", "OpenCV," and "matplotlib." To provide all mentioned capabilities for the user through the UI, last least a five tab UI seems necessary. The related figure of this section is presented in Appendix A. Each of these tabs may include several different sub-tabs. These five tabs are:

1. Main tab,
2. Online monitoring tab,
3. Forecast tab,
4. Data analysis tab,
5. Online control tab.

The main tab includes the following sections:

1. Single-line diagram,

2. Microgrid status,
3. Instantaneous total generation,
4. Instantaneous total load,
5. Power exchange at POI,
6. Instantaneous total renewable generation.

The single line diagram shows the current topology of the medium voltage network and connected DERs. Instantaneous total generation, total load, total renewable generation sections are providing corresponding real power (P), reactive power (Q), and power factor (pf). All values are presented in actual and per unit. Microgrid status shows the current operation mode of the microgrid and the operating frequency of the microgrid. In the background, when this tab is opened in the background, the server will send an administrative status check request every 10 seconds. With the information given by MCCD, the topology of the system will be updated. The resultant main tab design is presented in Figure A.1.

In the online monitoring tab, all sub-tabs corresponding data are presented in tabulated data format. When this tab is selected, the database's latest data will start to be checked, and the most up-to-date values will be shown on the monitor. The online monitoring tab consists of bus bars, lines, and smart assets (SA) sub-tabs shown in Figures A.2, A.3, and A.4. Pieces of information presented in these sub-tabs are given in Table 2.4.

The forecast tab lets the operator observe the corresponding plotting to renewable generation forecasts and load for the next 24 hours. Moreover, the user will be able to export the forecast data. It should be noted that the historical forecast data cannot be reached from this tab. When this tab is opened, the latest forecast results will be copied to local variables, and the graphs will be plotted using these local variables. This tab is shown in Figure A.5.

The data analysis tab is provided to explore, plot, and export the stored data for the determined time interval. The user determines the acquired time through the corresponding fields. The corresponding sub-tabs are bus bars, forecasts, lines, and smart

Table 2.4: Description of sub-tabs of GUI's online monitoring tab.

Sub-tab	**Information**
Bus bars	Voltage magnitude, voltage magnitude (per unit), voltage phase angle, injection current magnitude, injection current phase angle, real injection power, reactive injection power, apparent injection power, ON-OFF status if a device connected to bus-bar, power factor
Lines	Current magnitude, current phase angle, real power flow, reactive power flow, the status of the corresponding CBs, apparent power flow
SA	Timestamp of last received data package from MCCD, request ODBIT and IDBIT from MCCDs, last recorded locations of MCCD, Status of the MCCD, SOC of BSS, SOC of connected EVs' batteries

assets (SA). Bus-bars, SA, and Lines sub-tabs provide the historical records of the same data described in the online monitoring tab. Forecasts sub-tab enable the user to access the stored forecasted values for the selected unit's generation or load within the determined time interval and comparison with the actual values. Corresponding sub-tabs are shown in Figures A.6, A.7, A.8, A.9, and A.10.

The MGCS operations in the Table 2.1 are classified into manual and automatic. However, some operation is considered in both classes, and some of the operations can be selected by the system operator, whether an automatic or manual. The online control enables the user to perform manual control operations and determine some operations manually or automatically. Users can open and close the switches if they want. When the user selected this operation, the server will send the required Digital administration instructions to the MCCD. Depending on the received information (Digital administration reply), the online diagram will be updated. It enables MGO to execute unplanned islanding. Also, adjustable parameters of the control function, such as the POI power exchange setpoint and time for planned islanding, can be modified. In automatic control, the user can select the optimization algorithm. This can be a rule-based MPC with 24 hours forecast, MPC with 12 hours forecast, or instant optimization. The online control tab's design is illustrated in Figure A.11 .

2.5 Summary

The proposed MGCS is defined, along with associated components and their interconnections. The need for a multi-thread server for this MGCS and associated implementation is described. Also, the compliance of the centralized controller with the IEEE 2030.7 standard is investigated. Database, communications, and graphical user interface modules are detailed in-depth.

CHAPTER 3

THE CORE-LEVEL FUNCTIONS

A central multi-thread server consisted of four components is proposed in the previous chapter. The control functions are consist of two levels, which are core=level and higher-level functions. In this chapter, the transition and dispatch fictions that belong to the core-level are developed and explained.

The MGCS includes the control functions that define the microgrid as a system that can autonomously manage itself, either in islanded or grid-connected mode. It satisfies the interconnection requirements using functions at its function stack's high, core, or low level. The lower-level functions indicating DER/load/devices level functions are not considered in the proposed MGCS since related control actions are performed via network components' local control.

Control system core level functions designate the microgrid as an independent autonomously controllable system satisfying the DSO and microgrid operator's requirements. The main aim of establishing this function is to have a functionality-driven controller emphasizing the modularity of MGCS. This feature is achieved via platform-independent interfaces. MGCS's functional framework determined by IEEE 2030.7 Std. [9] is shown in Figure 1.5. The functions designated as core functions in this standard pave the way for a modular design of microgrid control systems.

Two core functions are specified in this standard: the dispatch function and the transition function. The dispatch function operates on a longer time frame than the transition function of the microgrid, typically in minutes, compared to milliseconds for the transition function. The relationship and interaction between the dispatch and transition functions and control levels are illustrated in Figure 3.1.

In the present approach, dispatch rule is a set of rules for four dispatch modes which are:

1. Steady-state grid-connected mode (SS1),
2. Steady-state islanded mode (SS2),
3. Unplanned islanding (T1),
4. Planned islanding (T2).

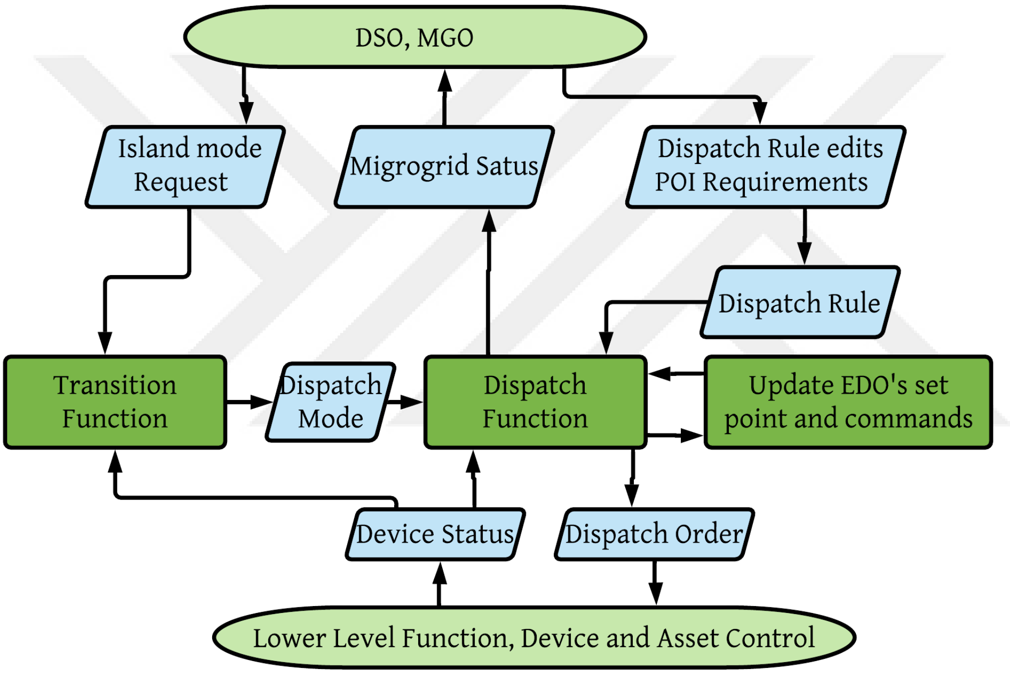

Figure 3.1: Relationship between the proposed transition and dispatch functions.

In this approach, the MG assets are a BSS, a DG, a PV system, a set of different loads, and a circuit breaker (CB) at the POI. The DG has a local frequency-droop (frequency- power) response [21], which is not dispatchable, which is the most common control scheme for DG. However, DG can turn ON/OFF via the MCCD. The BSS employs Vf control during islanded operation mode [44, 59], providing voltage and frequency reference for other assets' local controllers. The parameters related to the DG and BSS are given in Table 3.1. K_d and K_c are adjustable variables to determine minimum discharging and charging power, respectively.

Table 3.1: The parameters related to DG and BSS.

Asset	Parameter	Description
Diesel generator	t_{min}	Minimum DG ON time [s]
	t_{dg}	DG ON time [s]
	S_{dg}	DG status ON:1, OFF: 0
	P_{dg}^{min}	Minimum generation power [W]
	P_{dg}^{max}	Maximum generation power [W]
Battey storage system	SOC_{max}	The upper limit for SOC (%)
	SOC_{min}	The lower limit for SOC (%)
	P_{ch}^{max}	Maximum BSS charging power [W] $P_{ch}^{max} > 0$
	P_{dis}^{max}	Maximum BSS discharging power [W] $P_{dis}^{max} < 0$
	$K_c \times P_{ch}^{max}$	Minimum charging power [W]
	$K_d \times P_{dis}^{max}$	Minimum discharging power [W]

3.1 The Dispatch Function

The dispatch function computes and executes the dispatch orders, setpoints of DERs and controllable loads, and CB status based on dispatch rules. This function gets the MG operating mode and assets information from the transition function and MCCD, respectively. In summary, desired functionality of dispatch core function can be expressed as follows [9]:

1. During SS2, load, and generation are balanced,
2. During SS1 and SS2, controllable assets are re-dispatched in reaction to the internal events related to the load and generation status,
3. During SS1 and SS2, external commands and events, including MG operator and DSO, are handled, and controllable assets are re-dispatched if necessary.

Chu Sun et al. [44] developed a hybrid rule-based dispatch strategy as a microgrid central controller. The method keeps the BSS SOC around $50\%$for the sake of MG resiliency and reliability and to extend the BSS lifetime. Moreover, a dispatchable DG is kept ON during the operating modes of the MG. Three control modes for the dispatch strategy are allocated based on overlapped SOC ranges. In the proposed approach, a similar control allocation is adopted; however, the DG is not dispatchable, and it is off during SS1, and if necessary, it can be switched ON or OFF to decrease load shedding or renewable curtailment during SS2. Three SOC overlapped ranges are illustrated in Figure 3.2. Chu Sun at al. considered DG to be always ON in the first proposed rule-based dispatch function [44]. However,in the further study [42], the DG is tuned OFF by force-discharging dispatch rule during SS2 only considering the DG minimum ON time (t_{min}). The renewable curtailment or load shedding can be decreased by means of turning DG OFF or ON through all SOC ranges. Four adjustable parameters (SOC_{dl}, SOC_d, SOC_u, and SOC_{ul}) are used to define SOC ranges. Each SOC range corresponds to a control rule, which are force-charging, power-smoothing, and force-discharging. This control allocation logic is applied by dispatch function in SS2 (Conditions A, B, and C) and SS1 (A', B', and C'). In the algorithm shown in Figure 3.3, another parameter named as latch is utilized to avoid rapid control mode switching in the boundaries of SOC ranges shown as gray-colored areas in Figure 3.2. Control rules in both SS1 and SS2 are determined considering the imbalance between the load and renewable shown in equation (3.1) alongside the limits of all assets of MG, which are given in Table 3.1 and subsection 3.1.1. Moreover, the prioritized load management strategy is designed and utilized in the SS2 dispatch function.

The dispatch rules associated with SS2 dispatch mode are illustrated in Figures 3.4, 3.5, and 3.6 . The commands of dispatch rules will be cited by corresponding, blue-colored labels in mentioned figures. In these dispatch rules, the first priority is to define the power setpoint of BSS regarding the SOC ranges, which makes BSS avoid discharge and charge in force-charging and force-discharging conditions, respectively. The second priority is to prevent renewable curtailment and load shedding. Since load is dependent on people's instantaneous choices, it may be chaotic in remote systems. Load shedding is not recommended because one of the primary goals of microgrid operation is to offer consumers uninterrupted service.

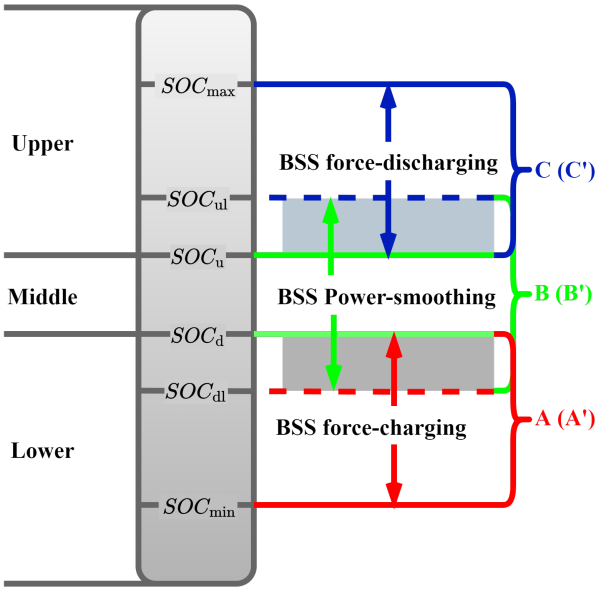

Figure 3.2: SOC ranges [44].

For the force-charging rule, given in Figure 3.4, the allowed operational interval of BSS and DG are given in equations (3.2) and (3.3). Considering these intervals, equation (3.5) is derived. This interval indicates the upper and lower limits of P_{miss}, in which load shedding or renewable curtailment is not necessary. P_{miss} is the power mismatch between the generation and load, which is to be compensated by the BSS. In the case of P_{miss}, being less than the lower boundary of equation (3.5), the operational status of DG has checked whether it is ON. If the DG is OFF, it will be turned ON (A2), then the BSS charging power will be minimum. Then the required amount of load to be shedded (P_{ld}^{shed}) will be determined (A3), and the OFF/ON command of DCLs and CCL's setpoints is determined through the load shedding procedure. Because of the discretely controlled loads, the shedded load might be more than the required amount, which will be checked by $P_{ld}^{shed,diff}$. If this variable equals zero, the process will be terminated; otherwise, this difference will be compensated by charging BSS or renewable curtailment.

$$P_{bal} = P_{ren} - P_{ld}^{tot} = P_{miss} - P_{dg} \tag{3.1}$$

$$K_c \times \; P_{ch}^{max} \leq \; P_{miss} \leq \; P_{ch}^{max} \tag{3.2}$$

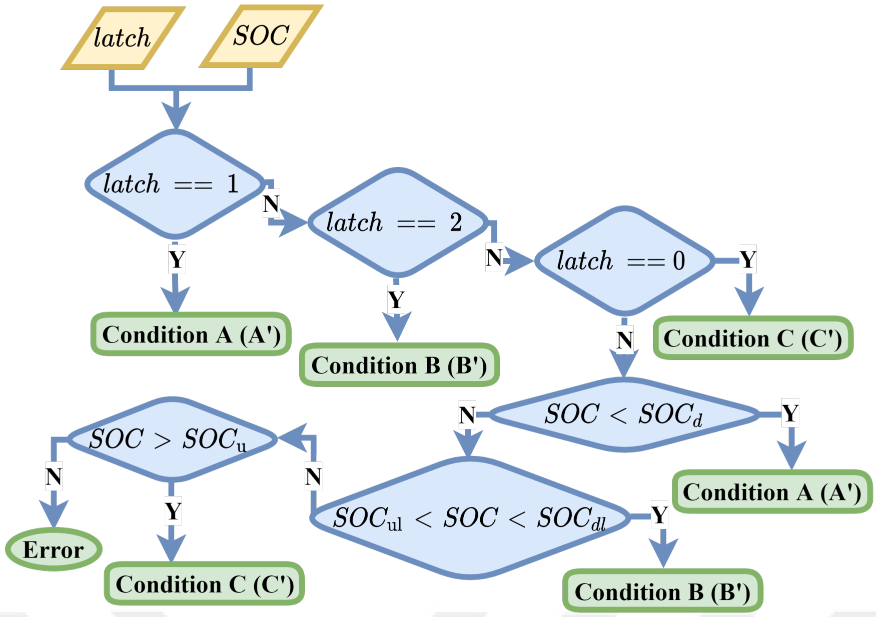

Figure 3.3: Control mode allocation algorithm.

$$P_{dg}^{min} \leq P_{dg} \leq P_{dg}^{max} \tag{3.3}$$

$$K_c \times P_{ch}^{max} - P_{dg}^{max} \leq P_{bal} \leq P_{ch}^{max} - P_{dg}^{min} \tag{3.4}$$

$$K_c \times P_{ch}^{max} - P_{dg}^{ris} \leq P_{miss} \leq P_{ch}^{max} + P_{dg}^{dec} \tag{3.5}$$

$$P_{dg}^{ris} = P_{dg}^{max} - P_{dg} \tag{3.6}$$

$$P_{dg}^{dec} = P_{dg} - P_{dg}^{min} * S_{dg} \tag{3.7}$$

If the P_{miss} satisfies the lower boundary interval presented in equation (3.5), and the restorable load (P_{ld}^{ris}), given in equation (3.8), is available, the load restoration procedure (A5) is executed to update the power and status set point of the loads. Additional to the generation and load imbalance, the possible BSS's share (P_{bss}^{ris}) in the incremental load (P_{ld}^{incr}) is $-K_c \times P_{ch}^{max}$ for this dispatch rule. It means that the minimum BSS charging power is reduced from the incremental load. After, execution of each of the load management strategy procedures, P_{miss} and P_{bal} values are updated. Then, the upper boundary interval given in equation (3.5) is checked. If this condition is fulfilled, considering the status and operational limitation of DG, BSS is charged as much as possible (A9, A11, and A12). DG is turned ON (A10) if it is necessary to fulfill this aim. However, if P_{miss} exceeds the upper boundary of the interval, renewables are needed to be curtailed, and BSS power setpoint is P_{ch}^{max}(A6, and A8). The DG might be turned OFF (A5), considering t_{dg} and t_{min} to avoid (A7) or reduce the renewable curtailment.

$$P_{ld}^{ris} = \sum_{i=1}^{N_{D1}} \left(\left(1 - S_{D1}^{i}\right) . P_{D1}^{i} \right) + \sum_{i=1}^{N_{D2}} \left(\left(1 - S_{D2}^{i}\right) . P_{D2}^{i} \right) + \sum_{i=1}^{N_{C1}} \left(P_{C1}^{max,i} - P_{C1}^{i} \right) + \sum_{i=1}^{N_{C2}} \left(P_{C2}^{max,i} - P_{C2}^{i} \right) \tag{3.8}$$

In dispatch rule B, shown in Figure 3.5, the average BSS power is zero, and DG power variations alongside (B3, B7, and B9) with DG status switching will balance the generation and load (B4 and B10). However, BSS and DG might not be able to compensate for the imbalance. Therefore, load shedding (B5) or renewable curtailment (B8 and B10) will be applied. Like dispatch rule A, load restoration procedure (B6) can be utilized depending on the assets' operational conditions. For this rule,P_{bss}^{ris} equals to P_{dis}^{max}, which does not mean BSS will discharge at maximum rate and P_{bss}^{spt} is determined in the further steps.

Similar to dispatch rule A, the force-discharging rule can be derived by applying interval analyses to equations (3.1), (3.2), and (3.9) reveals the interval given in equation (3.10). If P_{miss} does not satisfy the lower or upper boundaries of the interval presented in equation (3.10), load shedding (C3), and renewable curtailment (C10 and C11). Otherwise, P_{bss}^{spt} will set to discharge as much as possible (C5, C8, C9, and C13). However, DG might be turned ON (C2) or OFF (C12), considering t_{dg} and t_{min} to reduce load shedding and renewable curtailment, respectively. As main priority of this dispatch rule is to discharge the BSS, P_{bss}^{ris} is set to be P_{dis}^{max} for load restoration (C4).This dispatch rule is illustrated in Figure 3.6.

$$P_{dis}^{max} \leq \; P_{miss} \leq K_d \times P_{dis}^{max} \tag{3.9}$$

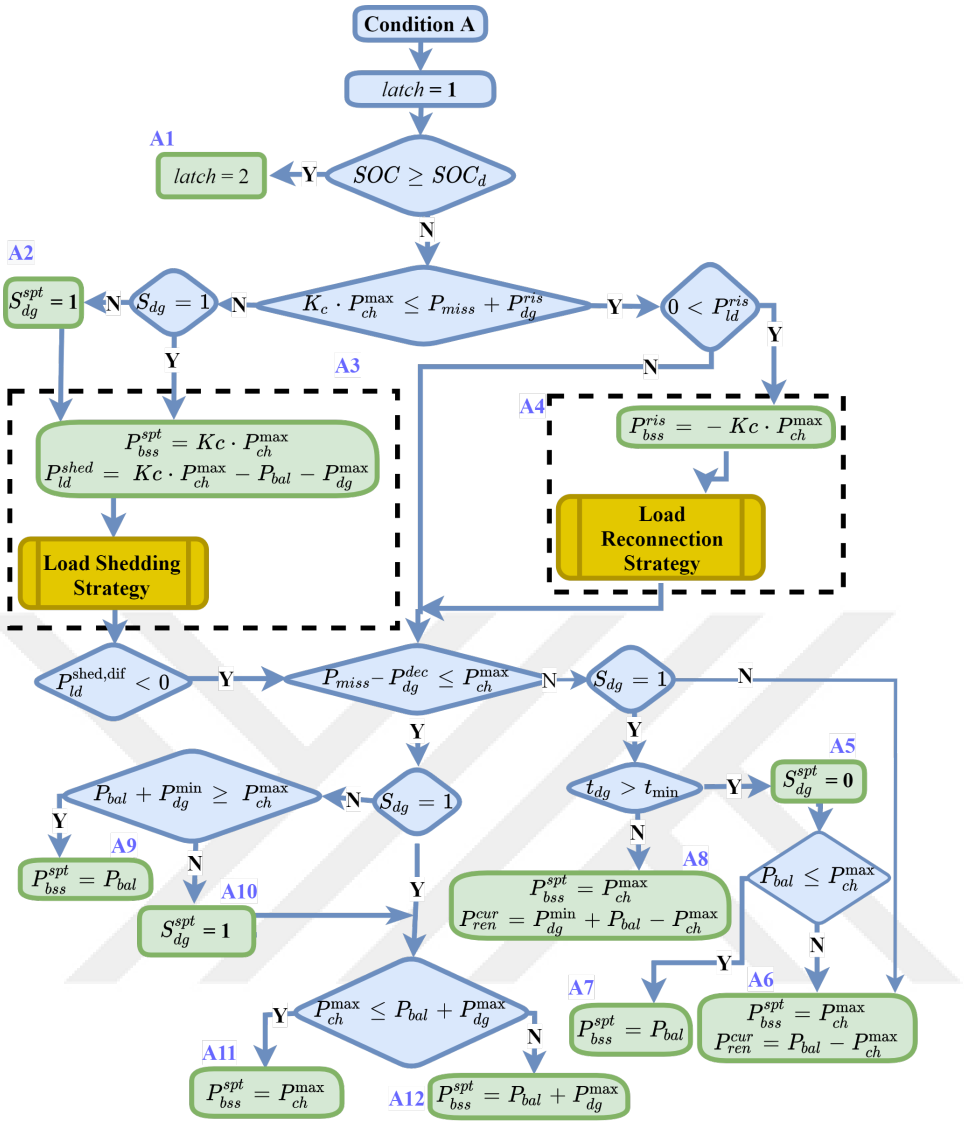

Figure 3.4: Force-charging control rule during SS2 based on the ranges of BSS's SOC.

$$P_{dis}^{max} - P_{dg}^{ris} \leq \ P_{miss} \leq K_d \times P_{dis}^{max} + P_{dg}^{dec} \tag{3.10}$$

The dispatch rules for SS1 dispatch mode (A', B,' and C') are illustrated in Figures 3.7, 3.8, and 3.9. The main differences between this set of rules with the previous set are that DG is kept OFF. Instead of load shedding, renewable curtailment, or load restoration, POI active power requirement (P_{POI}^{set}) is updated. For this purpose,

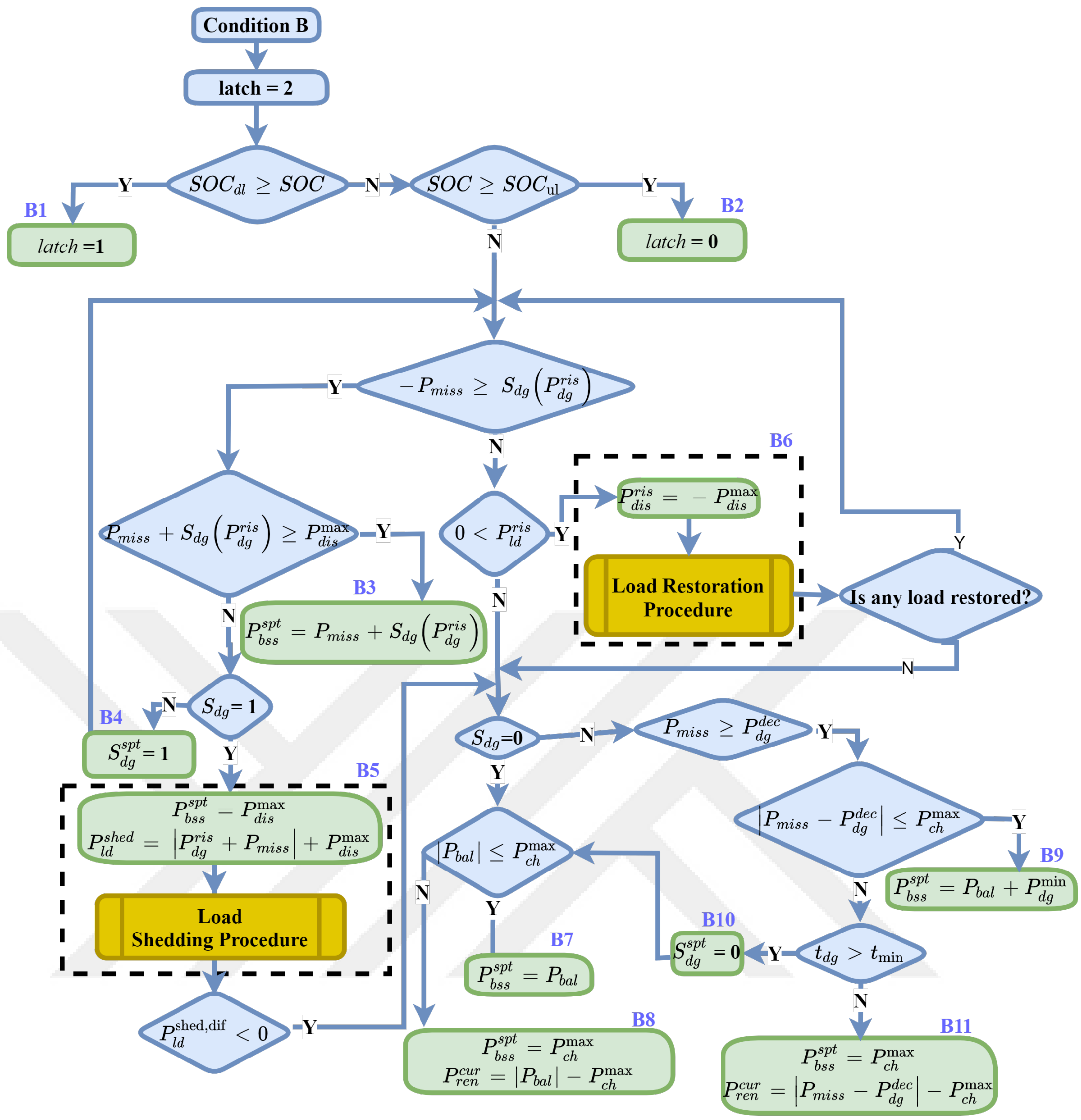

Figure 3.5: Power-smoothing control rule during SS2 based on the ranges of BSS's SOC.

equation (3.1) has been modified to equation (3.11) and equations (3.12), (3.13), and corresponding to A' and C,' respectively, are derived.

$$P^{*}_{bal} = P_{ren} - P^{tot}_{ld} + P^{set}_{POI} \tag{3.11}$$

$$K_c \times P^{max}_{ch} \leq P^{*}_{bal} \leq P^{max}_{ch} \tag{3.12}$$

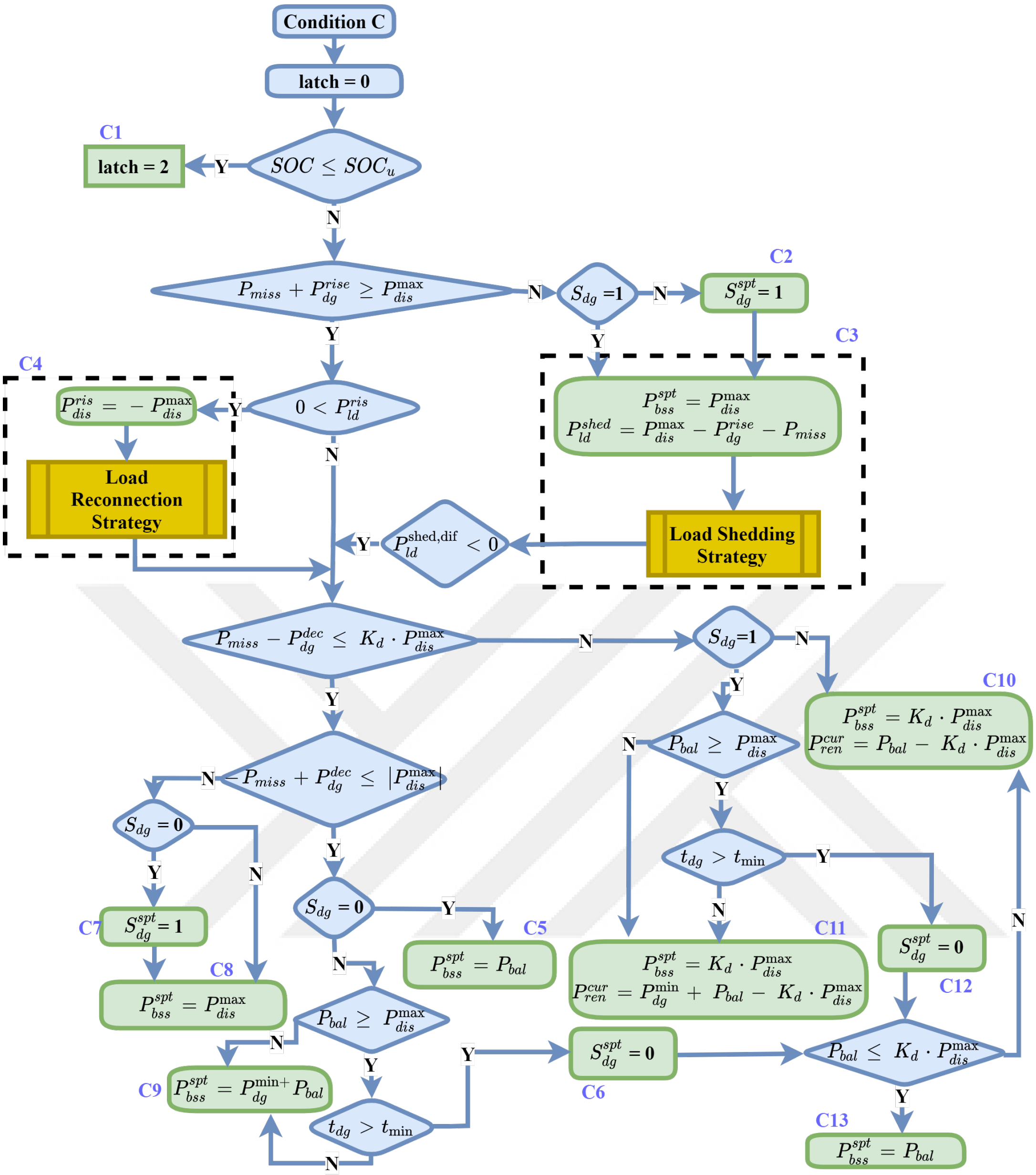

Figure 3.6: Force-discharging control rule during SS2 based on the ranges of BSS's SOC.

$$P_{dis}^{max} \leq P_{bal}^{*} \leq K_d \times P_{dis}^{max} \tag{3.13}$$

3.1.1 Load Management Strategy

The load of MG can be classified from two perspectives, criticality and controllability. In terms of criticality [14], loads can be categorized as follows:

1. Critical loads: These loads should be supplied in all normal operation modes of MG and cannot be shed (P_{ld}^{crt}).

2. Priority loads: These sets of loads can be shed or interrupted, but it is not preferred.

3. Interruptible loads: These sets of loads can be shed or interrupted at any time.

Besides, regarding controllability, loads can also be divided into two groups, discretely controlled loads (DCL) and continuously controlled loads (CCL).

Load management strategy consists of two procedures, which are load shedding and load restoration. Both of these procedures are designed regarding the criticality and controllability of loads. Increment or decrement in load might be due to the fluctuations of the renewable resources. Thus, modification is applied first on CCLs of the considered load category to reduce the ON/OFF actions impacts. Corresponding flow charts to these procedures are presented in Figure 3.10 and Figure 3.10, and details of related parameters are as follows:

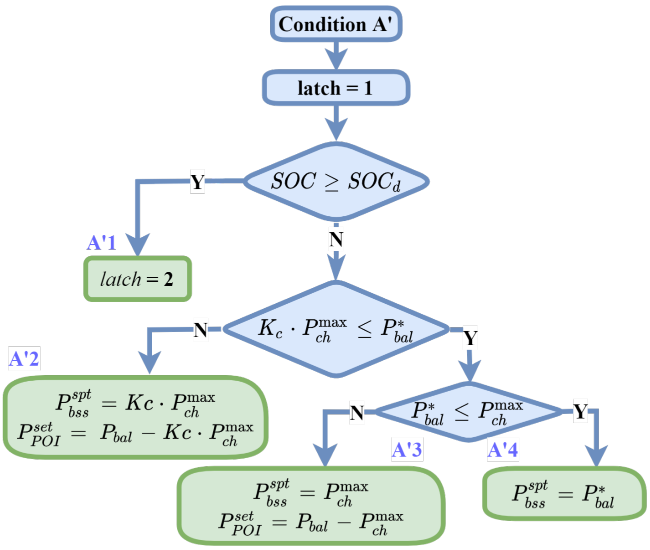

Figure 3.7: Force-charging control rule during SS1 based on the ranges of BSS's SOC.

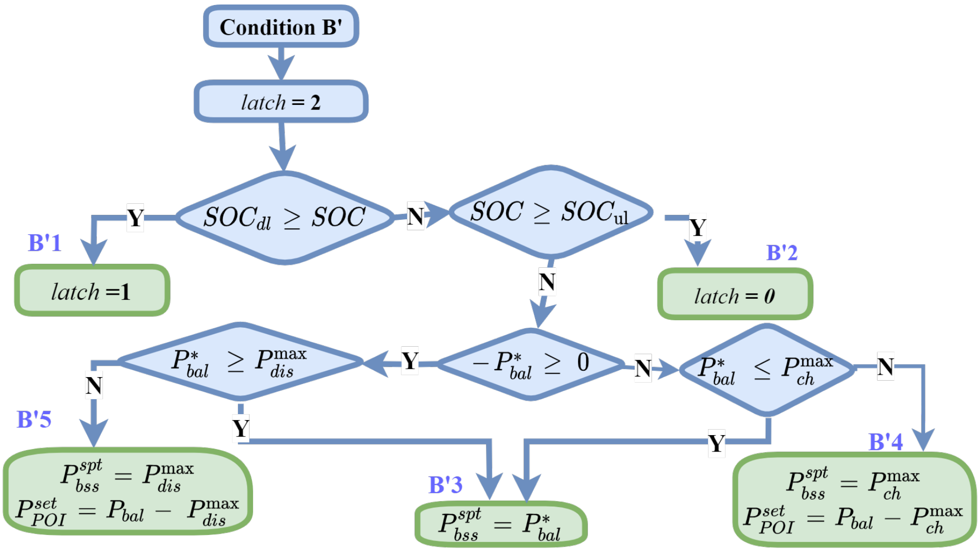

Figure 3.8: Power-smoothing control rule during SS1 based on the ranges of BSS's SOC.

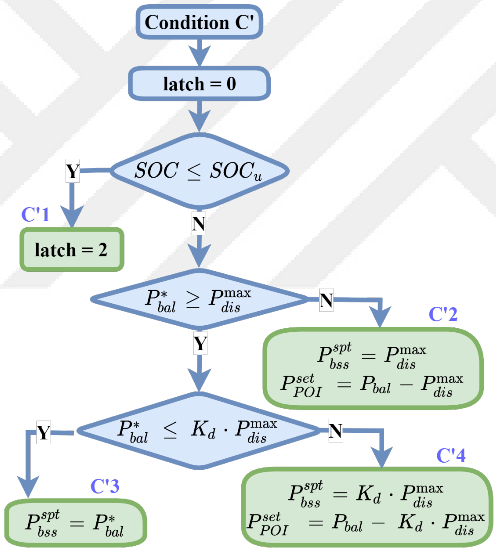

Figure 3.9: Force-discharging control rule during SS1 based on the ranges of BSS's SOC.

- P_{ld}^{tot}: Total load [W]

$$P_{ld}^{tot} = P_{crt} + P_{Dsh2} + P_{Dsh1} + \sum_{i=1}^{N_{C2}} P_{C2}^{i} + \sum_{i=1}^{N_{C1}} P_{C1}^{i} \tag{3.14}$$

- $P_{ld}^{sh,tot}$: Total sheddable load [W],

$$P_{ld}^{sh,tot} = P_{sh1} + P_{sh2} \tag{3.15}$$

- P_{Csh1}: Total sheddable interruptible CCL [W]

$$P_{Csh1} = \sum_{i=1}^{N_{C1}} \left(P_{C1}^{i} - P_{C1}^{min,i}\right) \tag{3.16}$$

- P_{Csh2}: Total sheddable priority CCL [W]

$$P_{Csh2} = \sum_{i=1}^{N_{C2}} \left(P_{C2}^{i} - P_{C2}^{min,i}\right) \tag{3.17}$$

- P_{Dsh1}: Total sheddable interruptible DCL [W]

$$P_{Dsh1} = \sum_{i=1}^{N_{D1}} S_{D1}^{i}.P_{D1}^{i} \tag{3.18}$$

- P_{Dh2}: Total sheddable priority DCL [W]

$$P_{Dh2} = \sum_{i=1}^{N_{D2}} S_{D2}^{i}.P_{D2}^{i} \tag{3.19}$$

- P_{sh1}: Total sheddable interruptible load [W]

$$P_{csh1} = P_{Dsh1} + P_{Csh1} \tag{3.20}$$

- P_{sh2}: Total sheddable priority load [W]

$$P_{csh2} = P_{Dsh2} + P_{Csh2} \tag{3.21}$$

- $P_{ld,C2}^{res}$: Total restorable priority CCL [W]

$$P_{ld,C2}^{res} = \sum_{i=1}^{N_{C2}} \left(P_{C2}^{max,i} - P_{C2}^{i}\right) \tag{3.22}$$

- $P_{ld,C1}^{res}$: Total restorable interruptible CCL [W]

$$P_{ld,C1}^{res} = \sum_{i=1}^{N_{C1}} \left(P_{C1}^{max,i} - P_{C1}^{i}\right) \tag{3.23}$$

- $P_{ld,D2}^{res}$: Total restorable interruptible DCL [W]

$$P_{ld,D2}^{res} = \sum_{i=1}^{N_{D2}} \left(\left(1 - S_{D2}^{i}\right).P_{D2}^{i}\right) \tag{3.24}$$

- $P^{res}_{ld,D1}$: Total restorable interruptible DCL [W]

$$P^{res}_{ld,D1} = \sum_{i=1}^{N_{D1}} \left(\left(1 - S^i_{D1}\right) .P^i_{D1} \right) \tag{3.25}$$

- N_{D1}: Number of interruptible DCL
- N_{D2}: Number of priority DCL
- S^i_D: ON/OFF status of i^{th} DCL
- $S^{spt,i}_D$: ON/OFF status command for i^{th} DCL
- N_{C1}: Number of interruptible CCL
- N_{C2}: Number of priority CCL
- $P^{spt,i}_C$: Power setpoint for i^{th} CCL [W]
- $P^{min,i}_C$: Minimum power of i^{th} CCL [W]
- $P^{max,i}_C$: Maximum power of i^{th} CCL [W]

It should be noted that the load management strategy is designed to be flexible, and the presence of any load is not necessary for this strategy. In these procedures, weighing methods given in (3.26) and (3.27) and queuing methods given in (3.28) are utilized to determine setpoints for CCLs and DCLs, respectively. Equation (3.28) is an optimization problem aiming to determine the ON/OFF status commands for DCLs such that the total power of that set load becomes less or equal to the desired value with the difference minimum difference. This optimization is utilized for both load shedding and restoration procedures. P_{plan} is positive for load shedding and is negative for restoration. Accordingly, the total shedded DCL might be more than the required amount. Therefore, in the case of partially shedding both CCL and DCL, it is supposed that all CCL is shedded (S3 and S8 in Figure 3.10). If the resultant shedded DCL is less than the desired, the mismatch is compensated by CCL (S5 and S10 in Figure 3.10).In the restoration procedure, a similar logic compared to the load shedding is obtained. Similarly, the CCL load is considered in this algorithm to avoid the rapid load switching due to renewable intermittency. However, the priority load group is restored first.

$$
\begin{aligned}
w_i &= \frac{P_C^i - P_C^{min,\, i}}{\sum_{i=1}^{N_C}\left(P_C^i - P_C^{min,\, i}\right)} \\
P_c^{spt,i} &= P_C^i - w_i.P_{plan}
\end{aligned}
\tag{3.26}
$$

$$
\begin{aligned}
w_i &= \frac{P_C^{max,\, i} - P_C^i}{\sum_{i=1}^{N_C}\left(P_C^{max,\, i} - P_C^i\right)} \\
P_c^{spt,i} &= P_C^i + w_i.P_{plan}
\end{aligned}
\tag{3.27}
$$

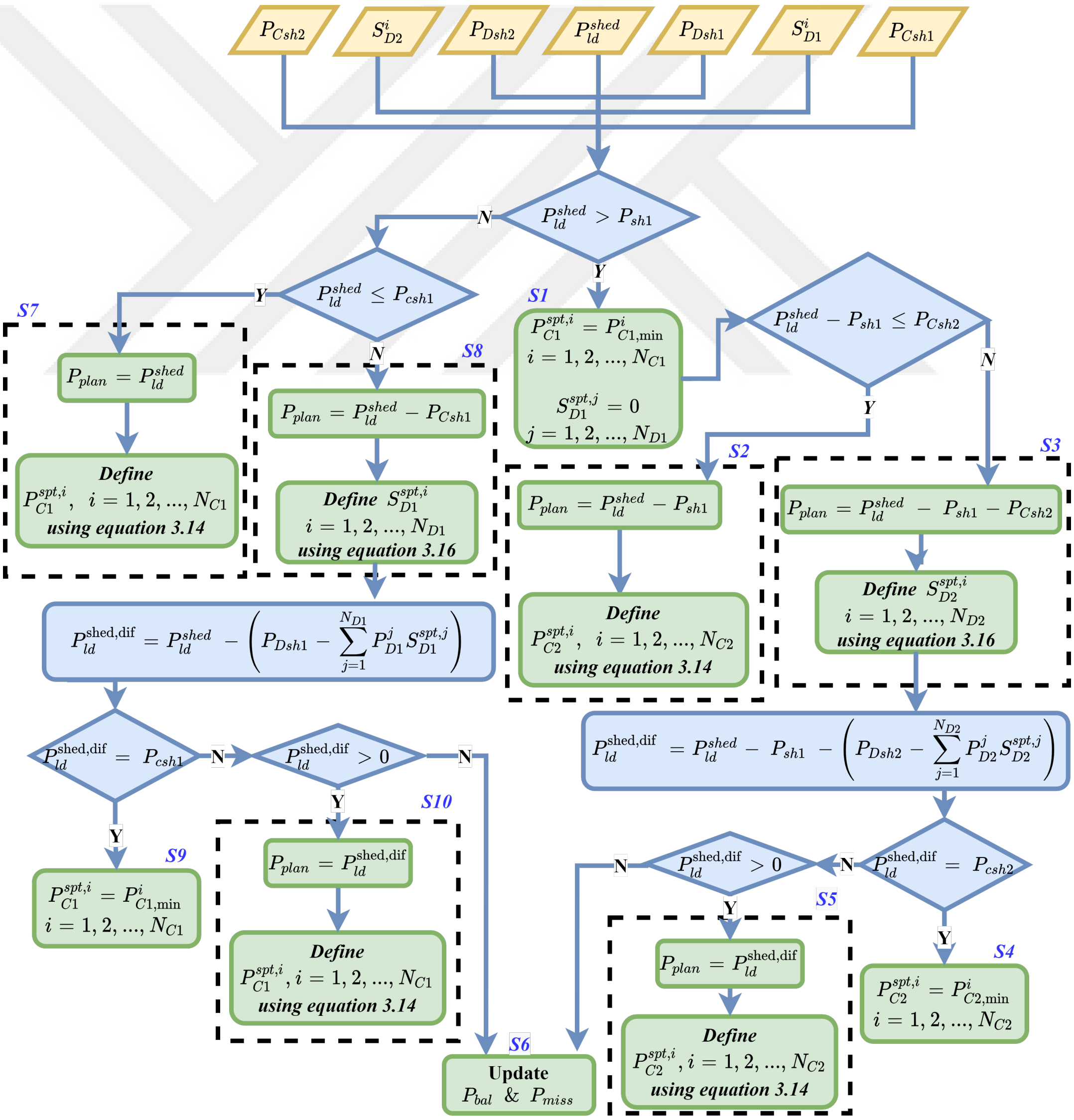

Figure 3.10: Flow chart of the load shedding procedure.

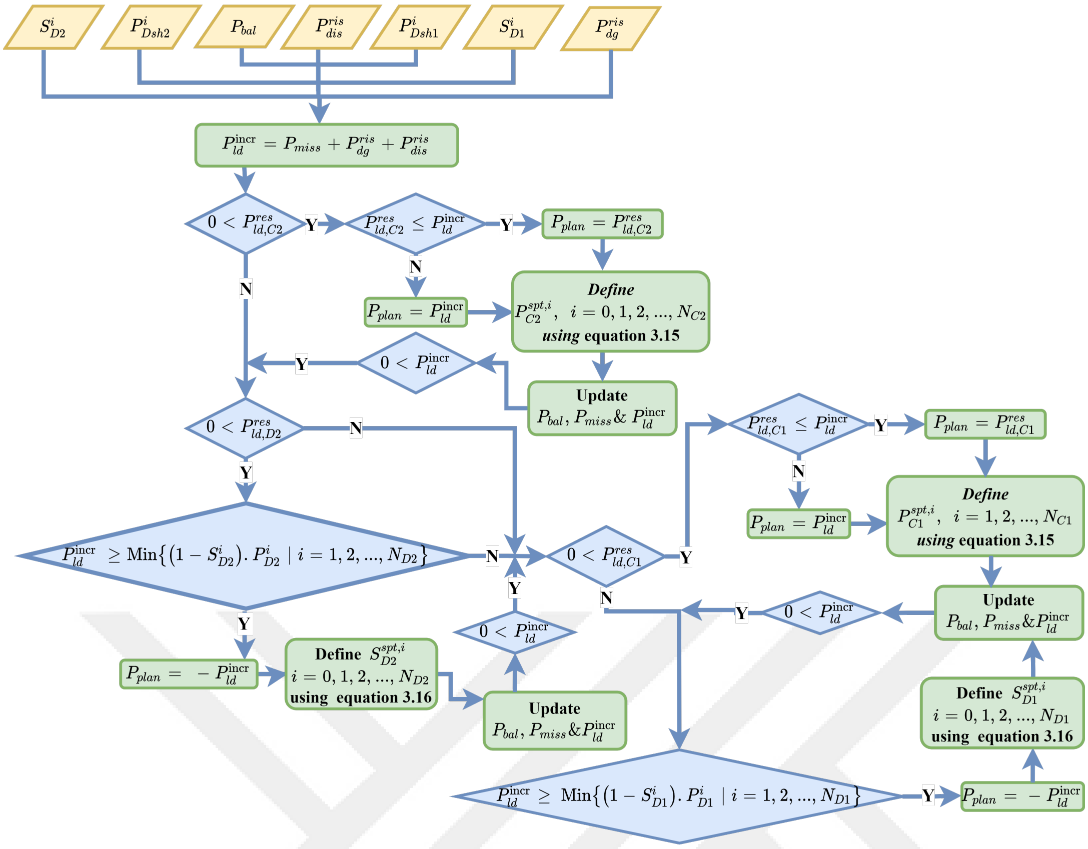

Figure 3.11: Flow chart of the load restoration procedure.

$$max \sum_{i=1}^{N_D} S_D^{spt,i}.P_D^i$$
$$S.t. : \sum_{i=1}^{N_D} S_D^{spt,i}.P_D^i \le -P_{plan} + \sum_{i=1}^{N_D} S_D^i.P_D^i \tag{3.28}$$

3.1.2 BSS State of Charge

During the operation of the microgrid, the stored charge in the battery constantly changes. To represent this behavior, the BSS should be modeled by using energy balance equations. This can be introduced in MPC by using constraints given in the algorithm 1. In this algorithm, t represents the time instantly. $E_{bss|t}$ is used to represent the stored energy in BSS at the beginning of time instant t. In the first part of the algorithm, which is the if-else part, the BSS energy is initialized. $E_{bss|int}$ is the initial BSS energy which considers a pre-defined time horizon. During the simulations, this value is stored after applying the control strategy in the previous real-

Algorithm 1 Algorithm of BSS SOC determination

if $(t == 0)$ **then**

$E_{bss|t} = E_{bss|int}$

end if

$E_{bss|t+1} = E_{bss|t} + \Delta T \times P_{bss|t}$

time step. However, for physical implementations, this value can be either estimated by using multiple redundant measurements as explained in [51] or retrieved from the battery management system if such data exist. Therefore, the second part of the algorithm ensures the energy balance of the BSS.

3.1.3 The Emergency Dispatch Order (EDO)

There is an exception for dispatching the MG assets. When the unplanned islanding event is detected, EDO will be executed directly by the transition function. Unplanned islanding, unlike planned islanding, makes it impossible to alter the DER controller set point or operating point in real-time. Because of the low inertia of power electronic converters, the voltage and current output of DER may experience substantial deviations in this circumstance. Therefore, this order is continuously updated as conditions change, and MG status is updated and is available for execution without waiting to be computed. The calculation process of this rule is shown in Figure 3.12. DG is off during SS1, and grid forming will be performed via BSS during SS2. Therefore, depending on the MG status, DG is turned on via EDO (E5). The presence of DG is not counted in load shedding (E4) because of the limited response speed of diesel generators.

3.1.4 EV Charging Management

In load management strategy, EV is considered as interruptible CCLs, and EV charging is managed during the SS2 by dispatch function. But, $P_C^{max,i}$ and $P_C^{min,i}$ related to these CCLs might change during the operation depending on the SOC of EV. For this purpose, storage of each EV is modeled separately, and two SOC range is considered for each EV. These SOC ranges are similar to the proposed ranges for BSS.

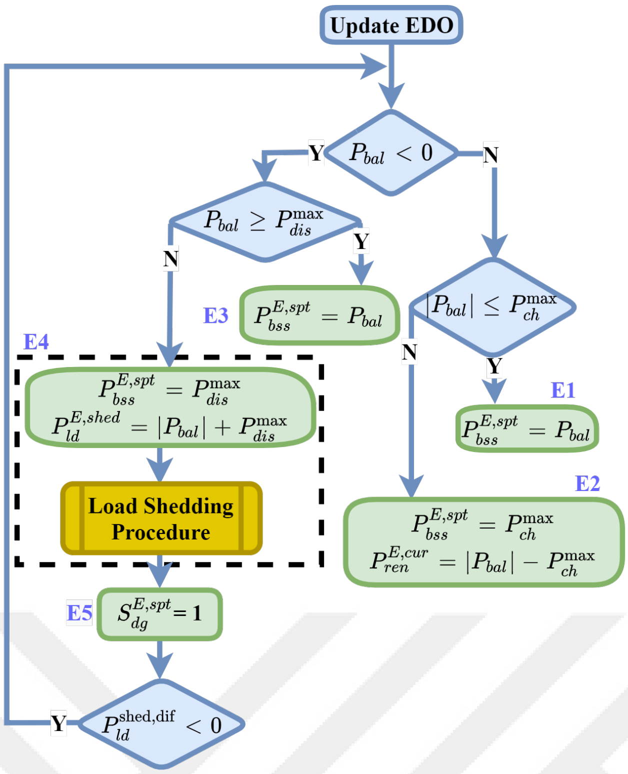

Figure 3.12: Emergency dispatch order calculation flowchart.

However, the power-smoothing mode is excluded. Considered SOC ranges for each EV are illustrated in Figure 3.13. SOC ranges include force-discharging (C_{ev}) and force-charging(A_{ev}). The gray-colored area is considered to avoid fast control mode oscillations.

The flow chart related to EV charging management is given in . Vehicle to grid operation is performed if there is permission from the related driver. If it is not allowed to get power from EV after entering the force-discharging region, EV's SOC will remain constant after entering the force-discharging region, and that EV will be excluded from the CCLs. However, for permitted ones, discharging is achieved by changing modifying $P_C^{max,i}$ and $P_C^{min,i}$ values. Related values of each control are described in Table 3.2. $P_{dis,ev}^{max,i}$ and $P_{ch,ev}^{max,i}$ are the maximum discharging and maximum charging power of i^{th} EV, respectively. In this way, corresponding power to the EV in C_{ev} mode will define a non-positive value within the load shedding and restoration procedures. This means EV will be discharged.

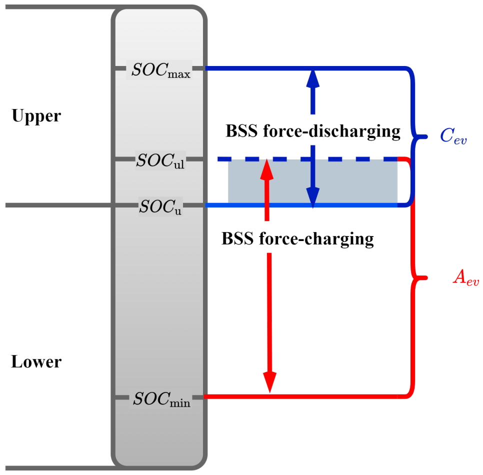

Figure 3.13: SOC ranges for each EV battery.

Table 3.2: Minimum and a maximum power of EVs as CCL in A_{ev} and C_{ev} control modes

Control mode	$P_C^{min,i}$	$P_C^{max,i}$
Force-charging	0	$P_{ch,ev}^{max,i}$
Force-discharging	$P_{dis,ev}^{max,i}$	0

3.2 The Transition Function

The transition function contains the logic for shifting the dispatch function between one of the essential dispatch modes to prevent or to delay a disconnection in a way that violates the interconnection requirement. In the recent approach, the transition function consists of planned and unplanned islanding transitions. The determined dispatch mode is fed to the dispatch function, and the dispatch function applies the dispatch based on this. However, during T1 and T2, the dispatch orders are executed by transition function, and dispatch mode returns to SS1 or SS2. In both T1 and T1, the POI CB will be opened, and BSS control will be shifted to Vf control mode by the transition function. The flowchart corresponding to this function is presented in Figure 12. The first step in this procedure is to check the status of POI's CB. Then, the planned islanding transition requirement is assessed. This process began to be obtained t_{isld} seconds before the planned time. t_{isld} is an adjustable variable depending on the response speed of the MG's assets. As the unplanned event is detected, the transition function will determine the assets' setpoints based on SS2 dispatch rules, and algorithms are given in Figure 3.3 and Figure 3.5. In this manner, the exchanged power at POI will be set at zero by implementing essential load shedding or renewable curtailment. Then dispatch mode will switch to SS2.

$$V_d = -\frac{2}{3}\left\{[\,V\}_a . \cos\left(2\pi f t\right) + V_b.cos\left(2\pi f t + 2\pi/3\right) + V_c.cos\left(2\pi f t - 2\pi/3\right)\right) \tag{3.29}$$

The MG remains connected to the grid if required criteria by DSO or MGO are satisfied[9]; otherwise, MG will be islanded. In this approach, unplanned islanding is achieved by monitoring the total active power, frequency, and voltage at POI. However, instead of three-phase voltage, V_d [60, 61]should be within the specified interval. V_d is calculated base equation (3.29), where V_a, V_b, V_c, and f are phase voltages and MG nominal frequency, respectively. In addition, unplanned islanding events could be initiate by external or internal command from DSO or MGO. If any of mentioned conditioned are satisfied, an unplanned islanding event will take place. In this regard, the calculated EDO will be executed by transition function immediately, then the rest of the required actions stated will be performed.

3.3 Summary

The proposed MGCS's core-level functionalities are presented. Dispatch and transition functions are included in this tier of functions. The dispatch comprises several rules, an emergency dispatch order, and a load management technique, all explained in relevant sub-sections. e

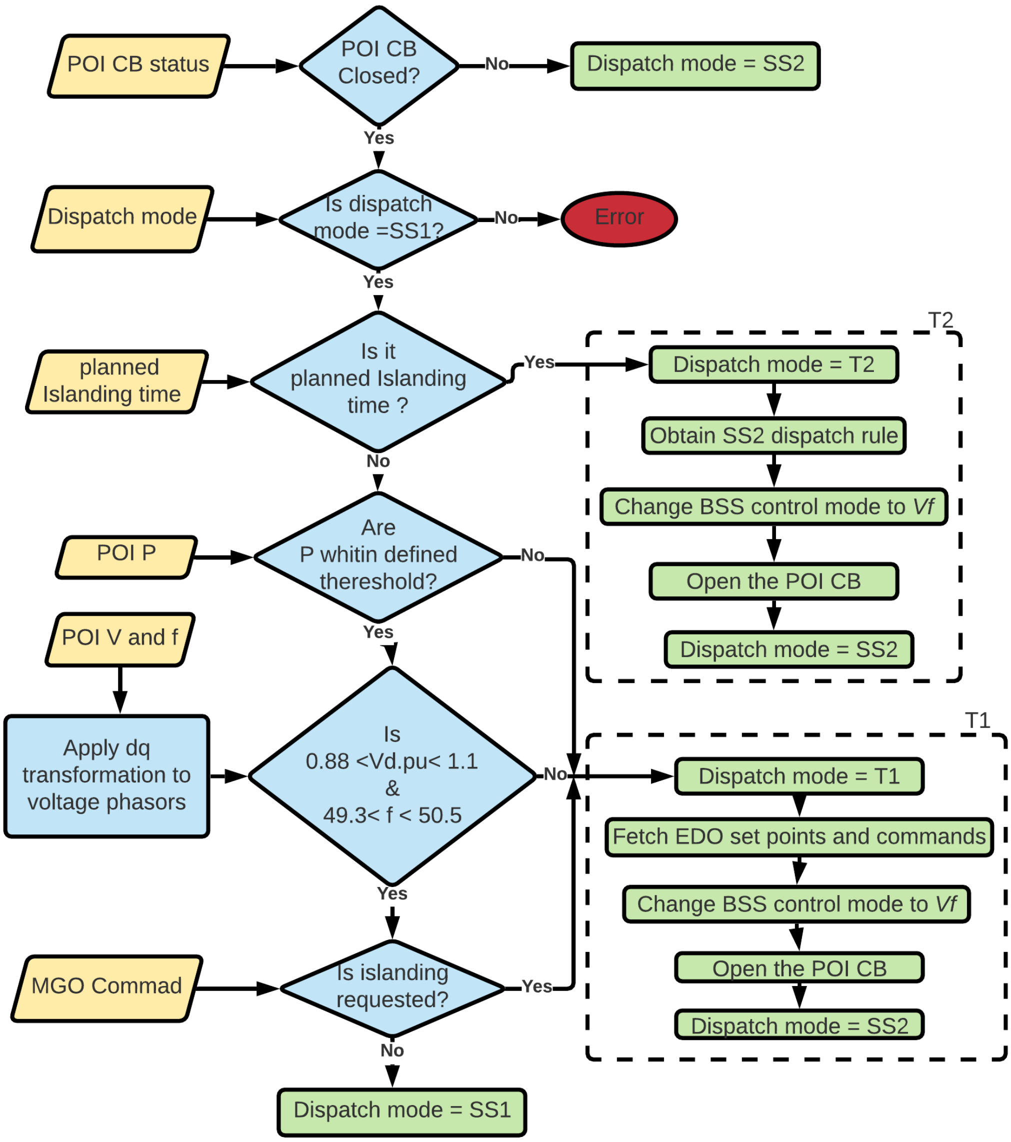

Figure 3.14: Transition function including T1 and T2.

CHAPTER 4

THE HIGHER-LEVEL FUNCTIONS

In microgrids, the intermittent characteristic of DERs creates some concerns about reliability. During the normal operation state of the grid, MGCS functions to minimize the operation cost of the microgrid. Also, the employment of V2G systems addresses new business models with new participants supporting service to vehicles, buying or selling electrical energy, and cooperating with utility grids. Electrical Vehicles participate in the microgrid central control strategies with various objects. Li et al. [52] presented an EV-based MPC algorithm to regulate the voltage. Frequency stabilization is maintained through MPC-based control of the microgrids with EV participation in [53] and [54], while MPC is utilized to manage the charging of parked EVs and BSS to achieve the optimized economical solution in [55]. In [51], in addition to the operation cost, the aging of BSS and EV batteries is also added to the cost function.

To achieve this, MPC and SMPC methods will be utilized as a higher-level function, which enables an optimum solution for long-term operation during the grid-connected mode. The SMPC method consists of multiple MPC runs. The details of the MPC algorithm can be found in [51]. The definition of MPC can be given as deciding the optimum control strategy for the current time instant based on the forecasted behavior of the system using dynamic models.

One of the most critical issues about the MPC methodologies is the correctness of the forecasts. This directly affects the performance of the method. The resultant forecasts generally lay in a probabilistic envelope, such as the PV forecasts, where the cloudiness level affects the predictions highly. Accordingly, these problems can be handled via a stochastic approach to the deterministic MPC method. Stochasticity will be added by using Monte Carlo Simulations (MCS); since this approach does not use any mathematically complicated models and still gives satisfactory results. For the PV generation, both the stochastic approach with MCS and the deterministic prediction approach with long short-term memory (LSTM) will be presented.

4.1 PV Generation Model

SMPC, require PV generation forecasts as input. For that purpose, in this work, two forecast methods are utilized. Firstly, LSTM will be introduced. Then, an MCS-based stochastic model will be proposed.

In literature, different artificial intelligence methods are used to forecast the PV power considering various effecting parameters. These methods can be examined under two categories: machine learning and deep learning (DL) methods [62]. According to several studies [62], in general, DL methods are considered effective and created more stable models. Recurrent neural networks (RNNs) such as LSTM can handle the information gained from former time steps of input data in the current time step. RNNs have loops that transmit information of one step to the subsequent steps in the network [63]. The feature that distinguishes LSTM from other RNN types is that it can learn long-term and short-term dependencies simultaneously effectively [64].

This study proposes an LSTM model, which predicts the next 24 hour PV generation in 15 minutes resolutions. In the proposed LSTM, 3-month PV generation time series, temperature, and cloudiness classification forecast data are used as inputs, which are updated daily. LSTM network consists of 128 hidden units. 80% of the available data is used as training data, and the remaining 20% of the data is used for testing. By using 3-month PV generation data, the effects of the seasonality and aging of the panels are eliminated. Resultant forecasts utilizing the proposed LSTM model are given in Figure 4.1.

For the second MCS-based method, global irradiation is used to create a probabilistic PV generation set. First, the possible maximum PV generation (PMPVG) is determined utilizing the PVLIB-Python [65] library for the considered PV array location and angle. The probabilistic generation scenarios for these arrays can be predicted

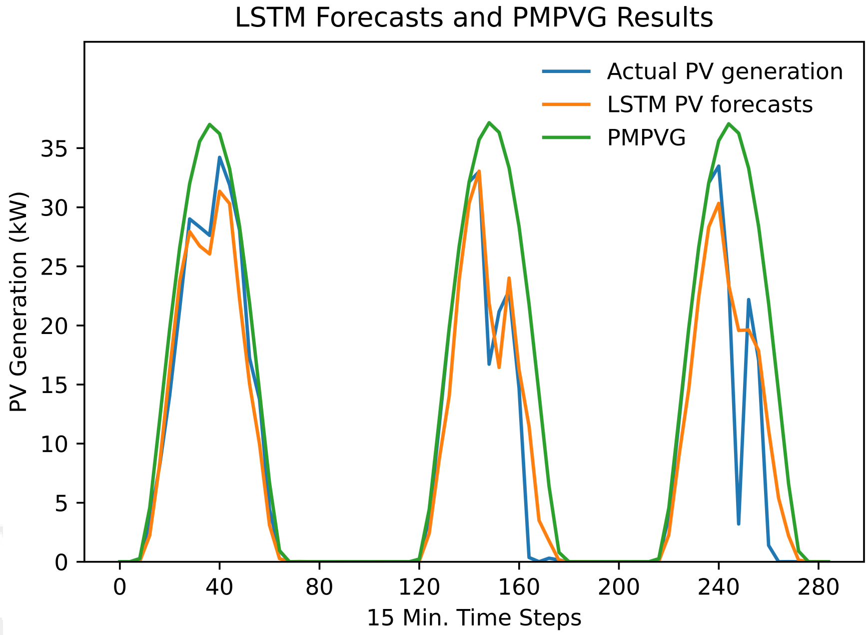

Figure 4.1: LSTM and PMPVG results

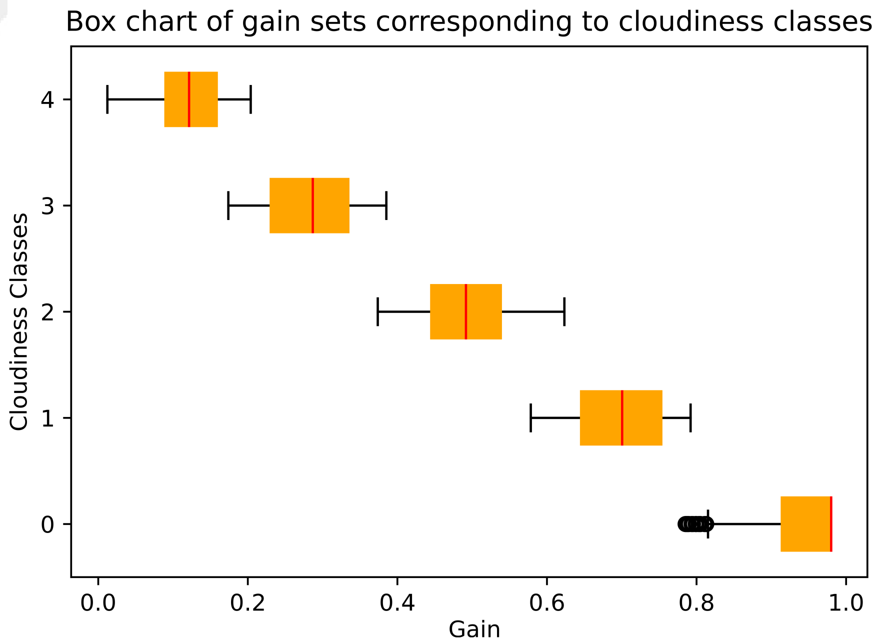

Figure 4.2: Box chart of gain sets corresponding to cloudiness classes

.

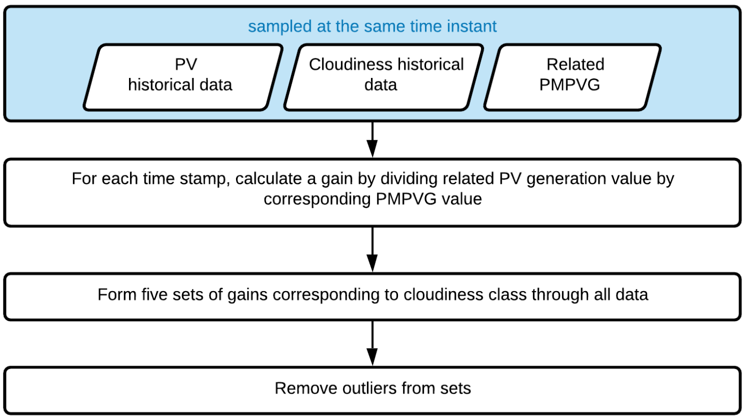

Figure 4.3: Flowchart of the gain calculation procedure

with the help of weather forecasts such as cloudiness classification data, where 0 for clear sky and 4 for a cloudy sky. For each scenario, the determined PMPVG is multiplied by a selected gain at each time step. This gain is randomly selected from the set of gains corresponding to that step's forecasted cloudiness class. The gains for each cloudiness class are defined according to the limited seasonal historical PV generation, cloudiness classification data, and related PMPVG. The corresponding flow chart to determine gains and box chart of gain sets corresponding to cloudiness classes are illustrated in Figure 4.3 and Figure 4.2, respectively.

4.2 Load Model

Load is an essential input of the proposed microgrid controller. Its estimation should be at a satisfactory level to get a proper result from the controller. Depending on the case, it may vary drastically during the day and be hard to predict with historical data. However, general industrial or commercial loads have a demand curve where the variance between two consecutive weekdays is low. Within this study's framework, the load and PV generation data of a research center are collected. Since this work aims to examine the stochastic nature of the input variables, and the daily demand pattern is similar throughout all days in the considered load data. The actual load data is used in the simulations. However, for the controller's actual implementation, a load forecast model is necessary. The load model predictions can be achieved in various ways, such as using LSTM [66], ANN, or Kalman Filter prediction step [51].

4.3 Control Strategy

The control strategy can be divided into two main parts, namely SMPC and MPC. In the following sub-sections, those will be separately described for the sake of full understanding. For each simulation time step, SMPC is run. In each SMPC, different scenarios are considered, and each scenario is simulated with deterministic MPC. In those MPCs, a MILP is solved by considering system models for a pre-defined horizon time.

While selling the excess power to the grid, a multiplication factor is used for the same prices. During the simulations, this factor is assumed to be 0.4.

4.3.1 SMPC

SMPC refers to a group of numerical optimization approaches to control stochastic systems constrained by the system states and inputs. SMPC can be beneficial to handle stochastic uncertainty with known probability parameters, and the constraints are naturally probabilistic [67].

In the simulations, two different algorithms are modeled. In the first algorithm, behaviors PV generation are modeled using MCSs (SMPC). In the second algorithm, the PV generation forecast is taken from LSTM (MPC). To evaluate the effectiveness of the SMPC algorithms, their results will be compared with the results of deterministic MPC algorithms. One uses actual measurements as inputs, and the other uses predictions as inputs.

In SMPC algorithms for the considered time step, all possible combinations of PV generation. After the call of each combination, an MPC algorithm runs, and the resulting decisions are stored. After running all MPC combinations, the median of the resulting BSS powers is selected. The EV powers that correspond to the median BSS power are also selected.

Although intuitive thinking may lead to using the BSS results' mean, the mean value may not coincide with an actual scenario. On the other hand, the median represents an actual MCS scenario. Moreover, with the selection of median value, the effect of outlier data in the stochastic process is eliminated. Another critical point is the selection of the BSS power as the main decision parameter. The reason behind this selection is, BSS is the only controllable and ready-to-use asset. At the same time, PV is not controlled since the inverters run a maximum power point tracker algorithm, and EVs may not be physically connected to the microgrid all the time.

It should be noted that the described procedure is applied for a single time step up to this point. After determining the SMPC result, the same process is repeated for the remaining simulation time steps.

4.3.2 MPC

MPC is an optimization-based control approach that minimizes the proposed cost function, which is given in (4.1) regarding the system's model and corresponding constraints within a specific time horizon. With this cost function MPC incorporates future reference information based on the generation and load forecasts into BSS and EV control problems to improve performance. Mixed-integer linear programming (MILP) is run to find the optimum power decisions, which satisfies all the constraints and minimizes the cost function given in (4.1). After minimizing the energy cost for the forecast horizon, only the decision corresponding to the first time step is applied to the actual system.

$$\begin{aligned} J = & P_G \times \frac{c_{buy}}{2} \times \left(\frac{P_G}{|P_G|} + 1 \right) \\ & + P_G \times \frac{c_{sell}}{2} \times \left(1 - \frac{P_G}{|P_G|} \right) \\ & + PF_{bss} \times |P_{bss}| + PF_{ev} \times \sum_{k=1}^{K} |P_{ev,k}| \end{aligned} \tag{4.1}$$

In (4.1), J represents the numerical result of the cost function for each MPC run, P_G represents a list of power decisions drawn from the grid throughout a single MPC simulation time, P_{BSS} represents a list of power decisions drawn from the BSS throughout a single MPC simulation time, and $P_{ev,k}$ represents a list of power decisions drawn from the kth EV throughout a single MPC simulation time. c_{buy} and c_{sell} represent the cost of the grid power when the power is bought from the utility and sold to the utility, respectively. Finally, PF_{bss} and PF_{ev} represent the penalty factors of BSS usage and EV usage, respectively. It can be seen that in (4.1), the main aim is minimizing the purchased electricity cost. Last terms with PF_{bss} and PF_{ev} are used to add the effect of battery aging and help to decrease harsh power fluctuations on batteries.

The details of the MPC algorithm can be found in [51]. Additionally, the effects of EVs are also included in the MPC algorithm in this work. The EVs are modeled as mobile BSSs, i.e., they are only used in time slots between when they enter and leave the microgrid. Each EV is modeled individually. Therefore, the power balance equation can be written as in (4.2) for the time instant t.

$$P_(ld)^{tot} = P_G + P_{ren} + P_{bss} + \sum_{k=1}^{K} P_{ev,k} \tag{4.2}$$

In (4.2), P_{ld}^{tot} and P_{ren} represent the power corresponding to loads, PV panels, respectively. During the operation of the microgrid, the stored charge in the battery always changes. To represent this behavior, the BSS should be modeled by using energy balance equations.

4.4 Summary

The fourth chapter deals with the higher-level function of the proposed MGCS. This set contains two alternative modelings for PV generation predictions and MPC and SPMC optimum dispatch methods. The stochasticity of PV generation is addressed in SMPC using Monte Carlo simulations. MPC also employs the LSTM for PV prediction modeling. These functions are suggested to control BSS, G2V, and V2G operations while keeping economic optimality in mind.

CHAPTER 5

SIMULATIONS AND RESULT

Simulation and tests related to the proposed microgrid control function are organized in two-part. The first part presents the core-level functions and performance within the different test scenarios recommended by the IEEE 2030.8 standard [22]. In the second part, as the high-level functions, MPC and SMPC control strategies are applied to the system with multiple cases to minimize the energy cost, and resultant costs are compared.

The considered system is presented in Figure 5.1, in which the positive directions of power flows are illustrated. The actual PV power generation and load data are collected from the university campus.

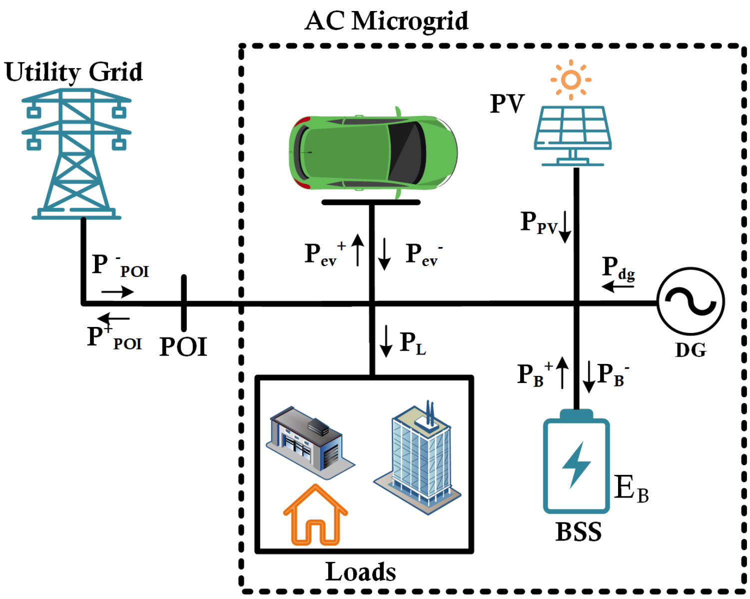

Figure 5.1: The scheme of the considered microgrid for simulations: illustration of MG boundaries and positive power directions.

Table 5.1: Parameters of the considered system for tests related to the core-level dispatch function

Parameter	Value	Parameter	Value
t_{min}	600 s	BSS energy capacity	350 kWh
P_{dg}^{min}	2 kW	SOC_{min}	20 %
P_{dg}^{max}	50 kW	SOC_{max}	90 %
P_{ch}^{max}	10 kW	SOC_{dl}	35 %
P_{dis}^{max}	-10 kW	SOC_{d}	40 %
k_c	0.05	SOC_{u}	60 %
k_d	0.05	SOC_{ul}	65 %
N_{D2}	5	N_{D3}	3
N_{C1}	4	N_{C2}	3
$P_{C1}^{min,i}$	1, 1.5, 1.2, 0.5 kW	$P_{C2}^{min,i}$	1.5, 1, 1.4 kW
$P_{C1}^{max,i}$	8, 2.5, 6, 5 kW	$P_{C2}^{max,i}$	8, 6, 8.5 kW

5.1 Tests related to the core-level functions

In this section, the test results related to core-level functions are presented. Noncritical loads consist of both continuously and discretely controllable ones. The parameters related to the considered system for all cases except for case-D1 are presented in Table 5.1.

The primary purpose of forming cases is to cover all dispatch rules in both dispatch modes in various conditions. IEEE 2030.8 Std. [22] specifies tests to test the pertinent operation of the dispatch function. In this regard, three test cases are formed, and details related to the assets for each case are given in Table 5.2. Test cases are as following:

- Case-D1: This case is prepared to investigate the advantage of keeping the BSS around 50%. For this purpose, a dispatch rule regardless of BSS's SOC is utilized in which the determined BSS power can be any value greater and lower than P_{dis}^{max} and P_{ch}^{max}, respectively. The related flowchart of this rule is illustrated in Figure 5.2. The same system is considered for the proposed SOC following presented in the chapter 3and non-SOC following shown in Figure, 5.2and the results will be compared. The time step related to this test and the dispatch function is 5 minutes.

- Case-D2: In this case, the performance of the dispatch function in normal conditions during SS1 mode is tested. For this purpose, tests cover two sequential days to observe the control mode switching properly. The time step related to this test and the dispatch function is 5 minutes. The variance of load and renewable generation in the collected dataset is low from sunset to sunrise. Therefore, all tests are started from 5 AM. In addition, the initial required P_{POI} set to -100 kW.

- Case-D3: In this case, the consequent performance of the dispatch function to the start and stop of the largest load will be assessed. The duration of the test is 6 hours, and MG is in islanded mode. The time step related to this test and the dispatch function is 1 minute.

- Case-D4: This case is performed to observe the proper reaction of dispatch function to temporary loss of the PV system during SS2. The duration of the test is 6 hours. The time step related to this test and the dispatch function is 1 minute.

- Case-D5: In this case, DG is not connected to the system, where upper and lower boundaries of this are considered to be zero. The time step related to this test and the dispatch function is 5 minutes.

Table 5.2: Description of details of the test cases related to the core-level dispatch function

Case	**Initial *SOC***	**DG presence**	P_{ren} **[kW]**		P_{ld}^{crt} **[kW]**		**Noncritical DCL [kW]**	
			mean	**max**	**mean**	**max**	**mean**	**max**
D2	0.25 %	No	84.8	190	21.7	43	46.5	79
D3	0.55%	Yes	106	148.5	37.2	91.1	53.4	105.7
D4	0.7 %	Yes	85	148.5	32.3	35.2	84.2	102.2
D5	0.85 %	No	85	148.5	21.2	41.3	53.4	105.7

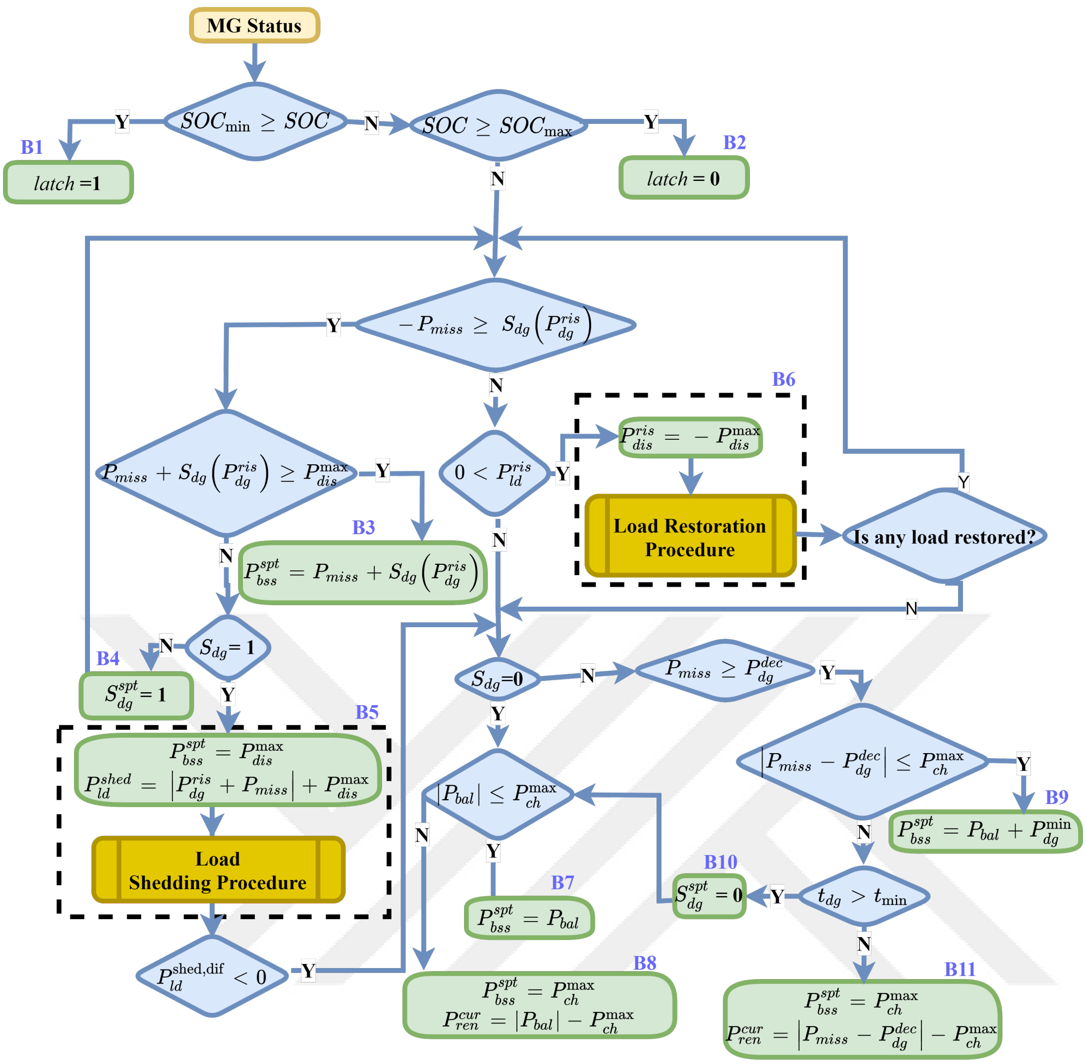

Figure 5.2: A non-SOC following rule-based dispatch rule.

The resultant simulations for case-D1 are shown in Figure 5.4. According to Figure 5.4a, When dispatch is fulfilled regardless of SOC, the BSS SOC has decreased to the desired minimum value. Therefore, BSS is not able to inject any power to MG, and support of the critical loads is completely dependent on the DG. This situation is caused by the reliability to supply MG's critical loads such that in case of DG failure, those loads will be shedded. On the contrary, the proposed dispatch function maintains to SOC around the 50% and avoids continuous discharge of BSS.

The results of case-D2 are illustrated in Figure 5.5. The initial SOC is 25% where makes the dispatch rule force-charging. However, the power exchange is less than the set value. Accordingly, BSS power is set to be the minimum charging power tile sunrise (8 AM). After sunrise, renewable power increases, which increases the P_{POI}

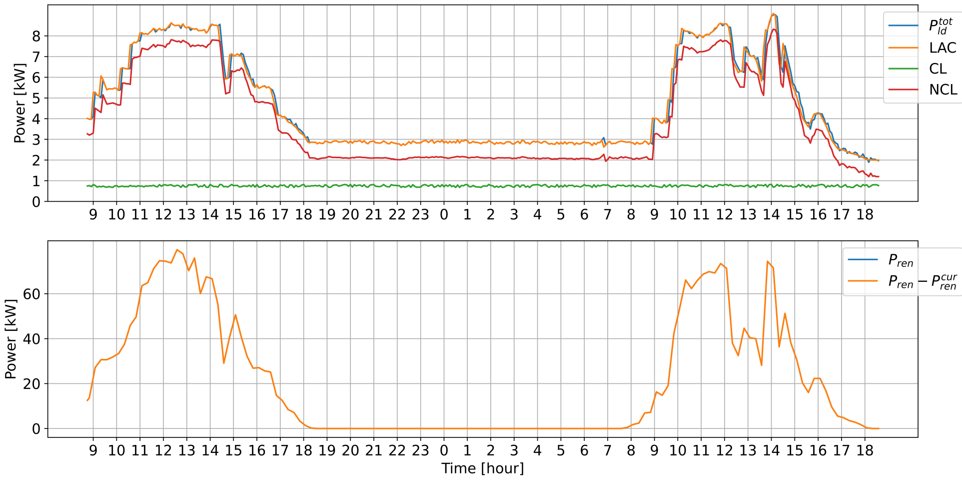

Figure 5.3: Simulation results for case-D1: The load and PV generation during the simulation considering non-SOC following dispatch rule.

up to more $-100kW$. Starting from this point, BSS power rises up to the maximum. As SOC crosses SOC_d, the control mode is switched to power-smoothing. After 10 PM, SOC enters the force-discharging region. Because of the zero renewable generations and defined dispatch rule, BSS is discharged at the minimum rate. In this test case, both aims are achieved to minimize charge-discharge cycles and avoid rapid control rule switching.

The Figure 5.6illustrates the test results of case-D3. In this test, 45 kW load, more significant than all other loads, is connected to the system at 11 AM and disconnected 30 minutes later. This load is considered as the critical load (CL) to avoid its shedding. Based on the Figure 5.6a, the necessary amount of noncritical load (NCL) is shedded to compensate for the generation and load mismatch immediately after the surge in load. Accordingly, available generation power, BSS discharge power, and load after control (LAC) are balanced. As can be seen in5.6c, a single interruptible DCL and both priorities and interruptible CCLs are shedded. It means that priority CCLs are shedded instead of shedding extra interruptible DCL. After a couple of minutes, shedded loads are restored as PV power output increases. Moreover, the Figure 5.6bshows that around 30 minutes before the event, DG power and BSS discharging rate have started decreasing in response to the rise of PV power output. Precisely after the event, both of these variables are set to corresponding maximums to minimize the load shedded load. The SOC remained within the power-smoothing range during the

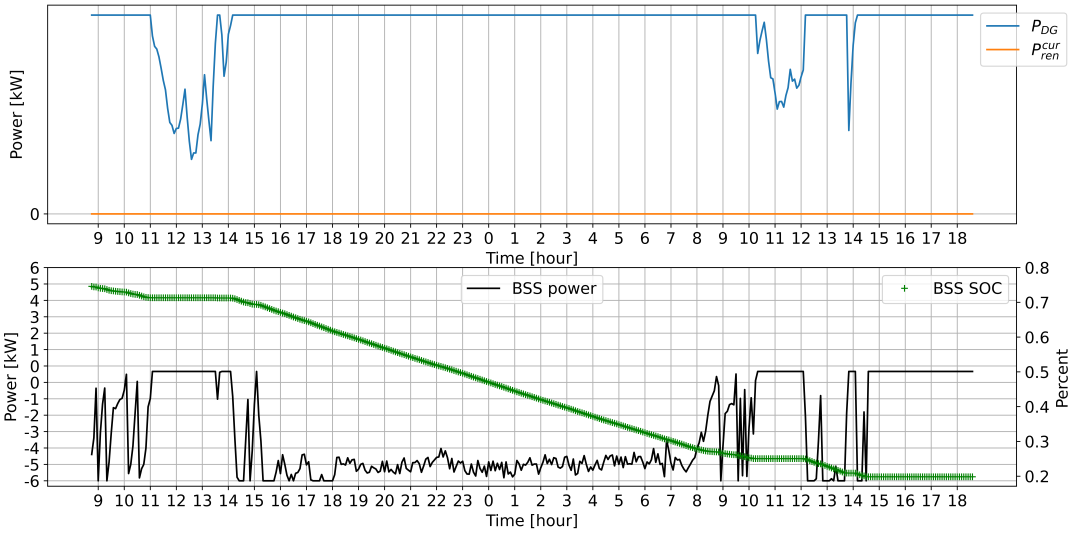

(a)

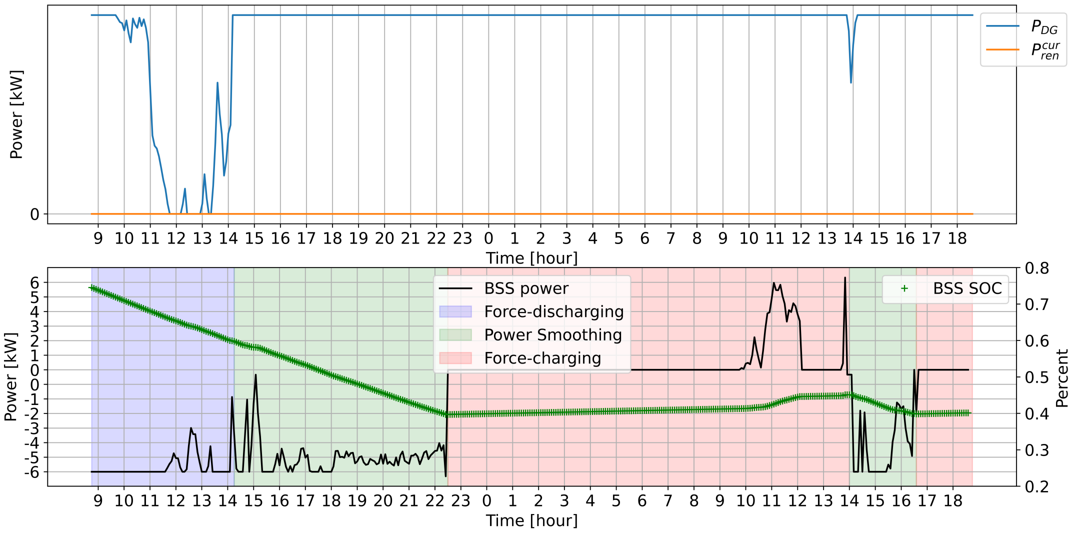

(b)

Figure 5.4: Simulation results for case-D1: (a) MG is dispatched by non-SOC following dispatch rule. (b) MG is dispatched by the proposed SOC following dispatch rules.

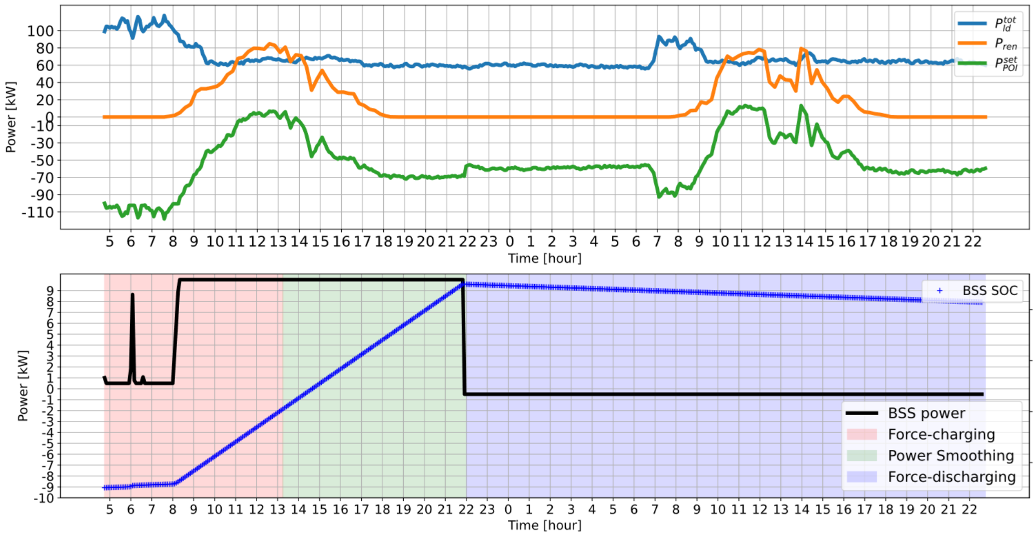

Figure 5.5: Test results for case-D2: MG in SS1 is tested for two days.

test. If the dispatch was force-charging before the event or because of the event, the power balance might fail. This issue entirely depends on the sizing of the MG assets and should be contemplated in MG planning.

The results of case-D4 are illustrated in Figure 5.7. The initial SOC is 70%, indicating dispatch rule force-discharging. The PV system is lost at 1 PM and returned to the system after an hour. Before this event, the DG is turned off, and even renewable generation is partially curtailed, and BSS discharging is at a minimum rate. Immediately after the PV system's tripping, the DG system is turned on and operated at maximum rated power. BSS discharging power increased, and the rest of the power mismatch is compensated by the shedding of NCL. The figreffig16b shows that interruptible DCLs and CCLs are shedded entirely. Then CCL are minorly are restored during the event in response to priority DCL and CL's variances. After the event ends, DG has turned off again, and BSS power is decreased.

The test results related to case-D5 are given in Figure 5.8. Within this test, DG is not available and generation and balanced via PV and BSS power. As the BSS is in force-discharging mode, its power output is set to maximum discharging rate up to around 10 AM, where renewable power significantly rises and event it is partially curtailed. Meanwhile, all possible loads are restored. However, In the case of a significant fall in PV power, load shedding is observed. According to this test, it can be deduced that MGCS can manage the MG without the DG.

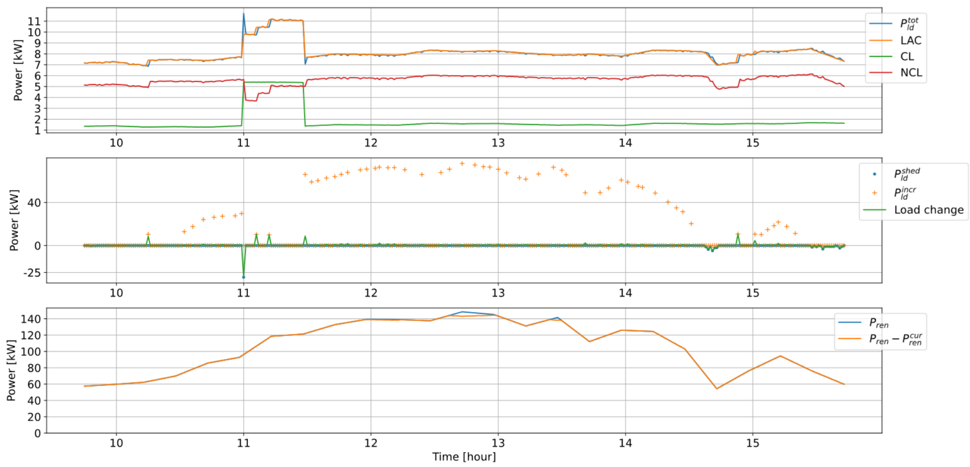

(a)

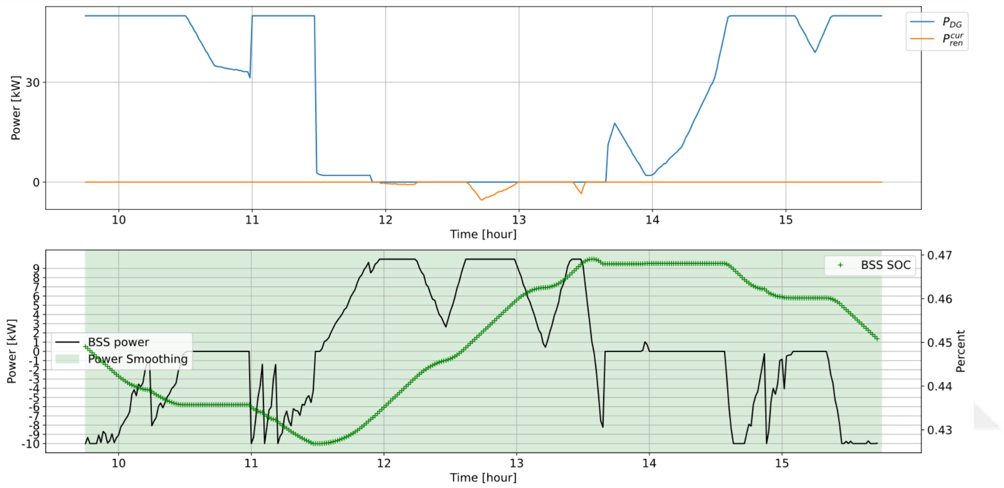

(b)

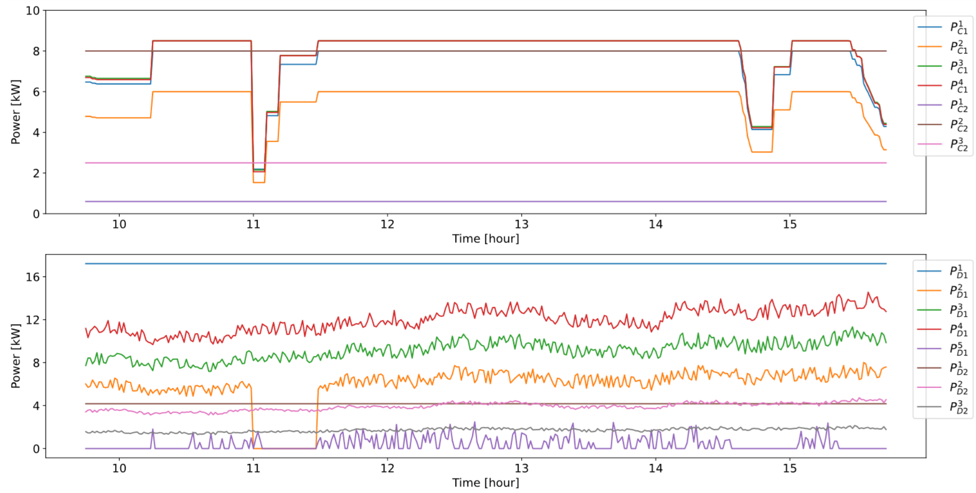

(c)

Figure 5.6: Test results of case-D3: A large load is connected at 11 AM for 30 minutes.

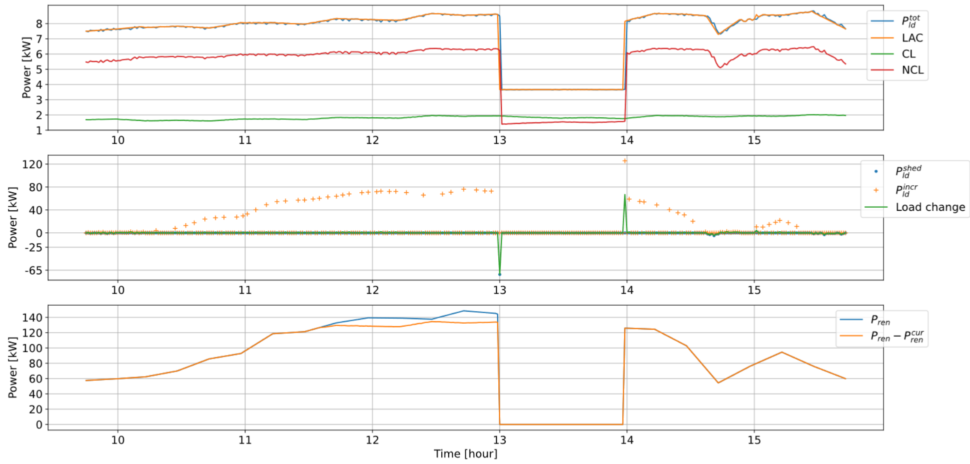

(a)

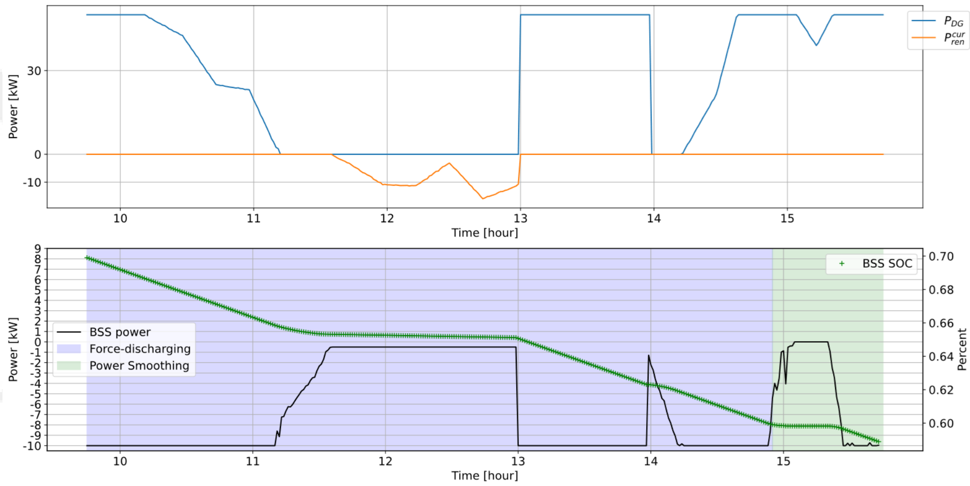

(b)

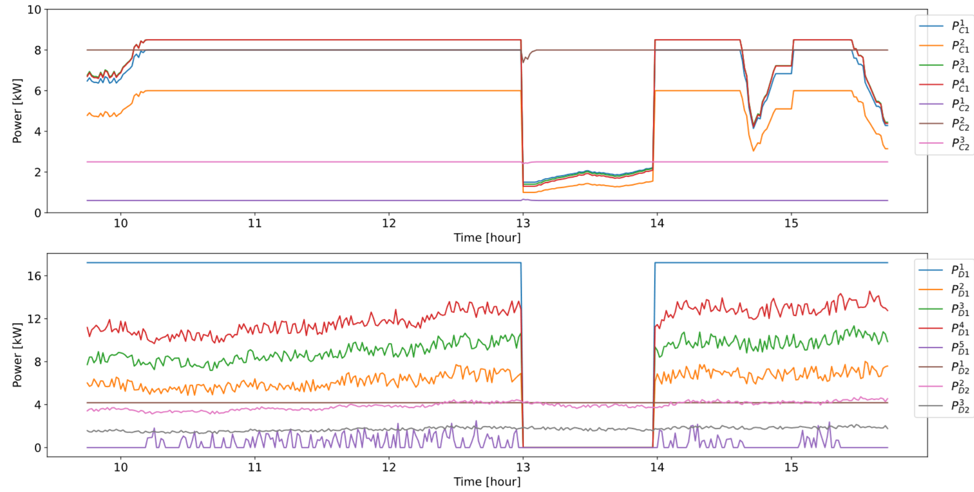

(c)

Figure 5.7: Test results of case-D4: The PV system is tripped at 1 PM for an hour

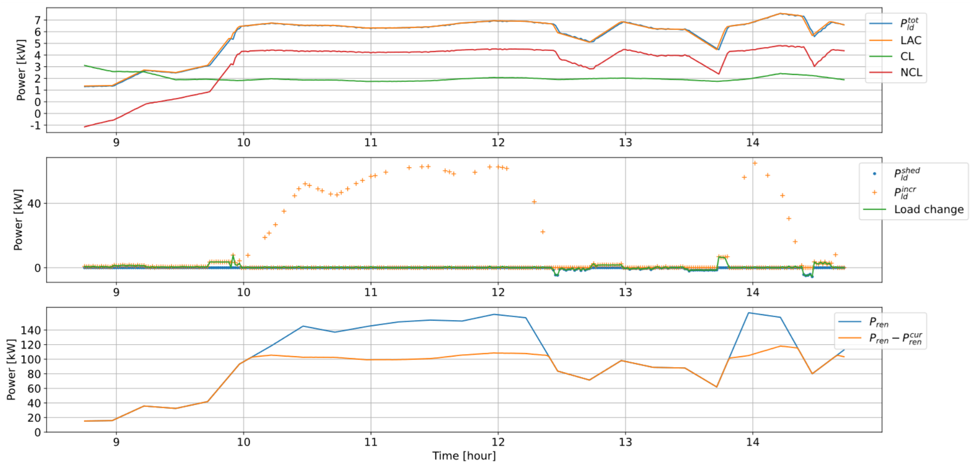

(a)

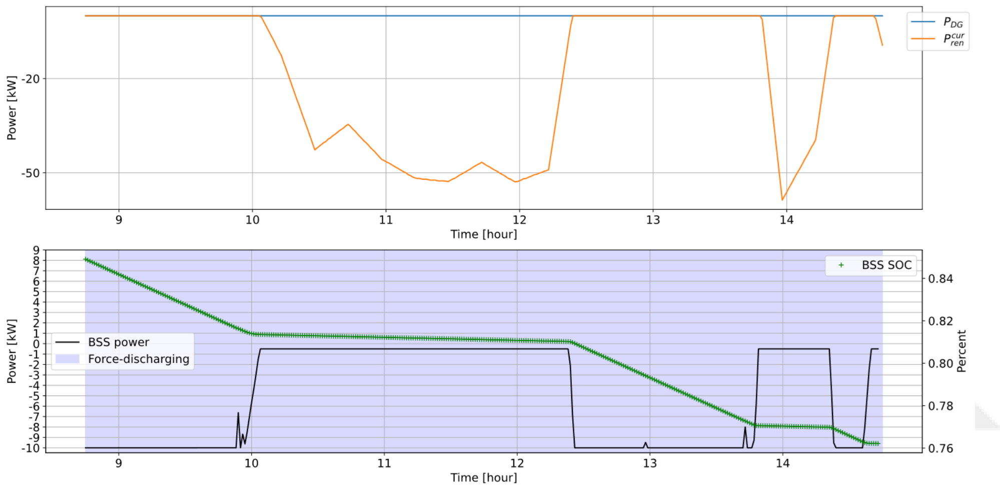

(b)

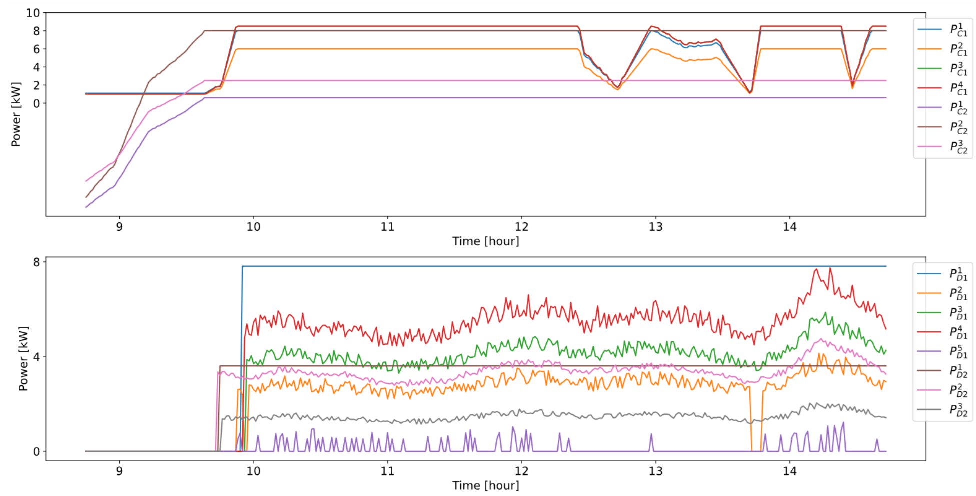

(c)

Figure 5.8: The results of case-D5: The DG is excluded from the system to test the dispatch function being generic.

5.2 Tests related to the higher-level functions

As mentioned before, higher-level functions are added to provide optimal dispatch of MG's assets. For this purpose, resultant energy costs for MG with different control function configurations are determined and compared. This study's data measured with quite variable weather conditions between March and May in Ankara, Turkey, are separated as 80 and 20 percent for training and tests datasets, respectively, for LSTM studies. Seasonality is discarded by limiting the considered period to spring. During the simulations, three-rate-tariff grid prices are assumed as follows:

- Day Tariff (06:00 - 17:00): 15 ¢/kWh,
- Peak Tariff (17:00 - 22:00): 30 ¢/kWh,
- Night Tariff (22:00 - 06:00): 8 ¢/kWh.

The results of different PV generation prediction strategies explained in the chapter 4, are given in Figure 5.9. In simulations, the prediction horizon is taken as 24 hours, and simulations proceed for 48 hours. The duration of a time step is taken as 15 minutes. A second system model is created by doubling the PV generation and PV predictions to examine the effect of PV penetration level. For simplicity, EVs are modeled as identical, i.e., EVs with 20 kWh capacity and 20 kW maximum charging power. BSS is assumed to have 350 kWh capacity and a 10 kW power rating. EV's entrance and leave time are 8 and 17:30, respectively. To examine the effect of renewable generation on the performance of the proposed SPMC, installed generation capacity

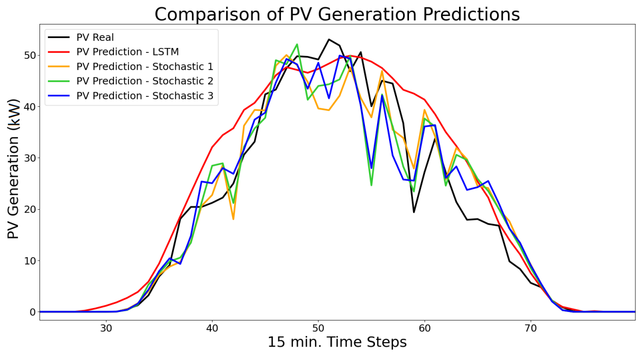

Figure 5.9: Comparison of different PV generation predictions

is assumed to be 55 and 110 kW. Penalty factors of BSS and EVs are calculated based on the method explained in [51].

In this work, four different cases are compared. In the first case, MGCS includes only core-level functions, and in the rest of the cases, multi-level control functions are considered. Considered methods and corresponding forecast inputs are explained below.

- Case-H1: The MGCS consists of only core-level functions: In this Case, set-points of MG assets are determined by the core-level dispatch function. The largest energy is expected in this case.

- Case-H2: The MGCS consists of MPC with actual data as the higher-level function: In this Case, actual PV generation data is fed to MPC. The best results are expected in this case.

- Case-H3: The MGCS consists of MPC with forecasted data as the higher-level function:: In this Case, MPC is fed with an LSTM forecast of the PV generation.

- Case-H4: The MGCS consists of SMPC with MCS scenarios for PV generation as the higher-level function: In this Case, PV forecast data are populated. The MCS method explained in the section 4is used to create PV generation scenarios.

In Tables 5.3 and 5.4different cases, their corresponding resultant energy costs (RECs) in terms of $, prediction performance measures are given. For the LSTM PV prediction, the resulting RMSE values are 5.603 kW and 11.206 kW for 55 kWp and 110 kWp generation capacity cases, respectively. The resulting power flows and energy levels of the main assets for Case-H4 with 75 PV-group scenarios can be found in Figure 5.10.

Table 5.3: Results of Case-H2 and Case-H3

Case	**REC ($)**
PV Generation Capacity~= 55 kWp	
H1	225.121
H2	187.601
H3	188.712
PV Generation Capacity~= 110 kWp	
H1	162.135
H2	134.145
H3	146.750

Table 5.4: Results of Case-H4

Number of MCS PV-Group	**REC ($)**
PV Generation Capacity~= 55kWp	
75	190.011
100	189.365
150	188.286
PV Generation Capacity~= 110 kWp	
75	143.253
100	144.053
150	**139.712**

The Table 5.3shows that Case-H1 and Case-H2 have the highest and lowest energy cost, respectively. These results were expected as expected since in Case-2, the actual generation data are used as input, and dispatch orders are calculated regardless of cost and forecasts. The MPC method's vulnerability can be seen in Case-H3; because the method's performance depends on the input forecasts' success. In Case-H3, the forecast errors cause an increase in energy cost.

The results of Case-H4 are given in Table 5.4 generally lies in between the energy costs of Case-H2 and Case-H3, which is also as expected. The stochastic nature of

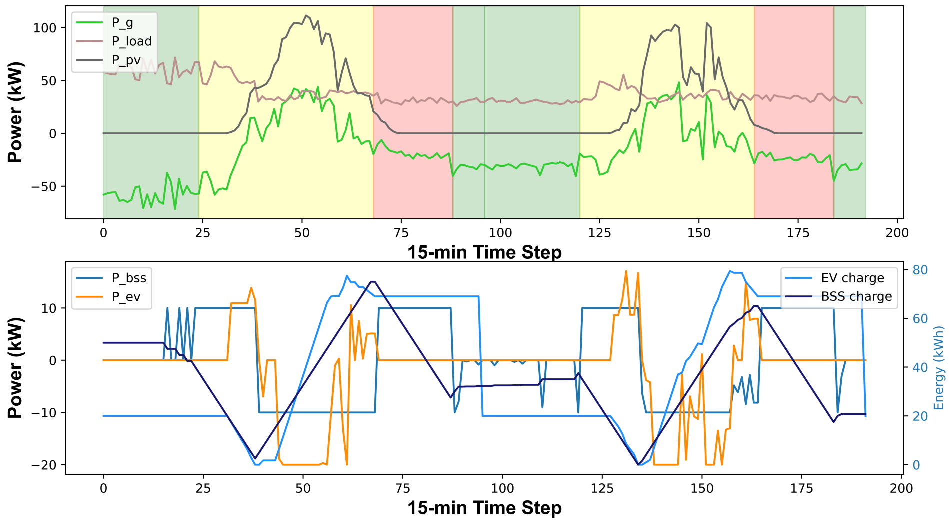

Figure 5.10: Power flows of microgrid assets for Case-H4 with 75 PV scenario, considering PV generation capacity = 110 kWp

the SMPC results can easily be caught because energy costs might be higher even if the stochastic scenarios increase.

It can be seen that the amount of renewable generation is another essential factor in the effectiveness of the control algorithm. When Case-H3 and Case-H4 are set side by side, these have similar results in low renewable penetration. However, when the renewable support increases, Case-H4 starts to give better results. As the PV prediction level increases, the effects of cloudiness increase. Therefore, the population of PV generation scenarios can better catch the actual PV generation. Based on Figure 5.9, LSTM may not achieve enough success in a day with high cloudiness fluctuations, especially in fast ramp-up and downs. From these results, it can be said that the stochastic population of PV generation can improve the results.

Therefore, the different share of renewable penetration can interchange the superiority of Case-H3 and Case-H4, i.e., a tailor-made decision should be taken according to the infrastructures in the microgrid.

5.3 Summary

The simulation test results of the proposed control function consisting of seven cases are given and discussed. Through the first set of tests advantage of SOC following logic, being generic, and the reliability of core-level dispatch function is shown. In the second section, the resultant energy costs for multi-level and single-level MGCS are compared. Also, the performance of the proposed SMPC and MPC are analyzed.

CHAPTER 6

CONCLUSION

In this thesis, a centralized microgrid controller is developed. This system is composed of the central multi-thread server (CMTS), which acquires the data from the filed units. Then, this information is processed, and CMTS executes consequent commands. The field units also apply the commands from the CMTS to the controlled assets.

The functionalities of the MGCS are compatible with IEEE 2030.7 and 2030.8 standards. The scope of the IEEE 2030.7 standard is to address the functions above the component control level associated with the proper operation of the microgrid energy management system that is common to all microgrids, regardless of topology, configuration, or jurisdiction. The CMTS includes four modules, including communication, database, graphical user interface, and control functions modules. These modules provide autonomous management of MG, online monitoring, data visualization, and manual operations by MGO. The communication framework among these system components is established through TCP/IP internet socket.

The generic MG control functions module has a multi-level framework consisted of core and higher levels. Dispatch and transition are the core-level functions. These platform-independent functions dispatch the MG assets with a BSS SOC-following logic. The primary purpose of this logic is to keep SOC around 50% for the sake of MG resiliency and BSS lifetime. The generic dispatch function is assembled by a load management strategy and dispatch rules that follow SOC. According to both criticality and controllability of loads, the load management method sheds and restores the specified amount of load. Because of these control capabilities, the proposed MGCS may be used in various microgrids, independent of their size or application.

Also, higher-level functions mentioned in IEEE 2030.7 such as load and renewable generation forecasts and optimal dispatch are adjoint with core-level functions. Stochastic model predictive control, model predictive control, PV generation forecasts with LSTM and Monte Carlo simulations are considered the higher-level functions of the proposed MGCS. The proposed LSTM model predicts the next 24 hour PV generation in 15 minutes resolutions. This model is trained with 3-month data to decrease the effects of the seasonality and aging of the panels. For the MCS-based method, global irradiation is used to create a probabilistic PV generation set. The MPC and SMPC are applied to the system to minimize the energy cost. The first strategy takes LSTM forecasts for PV generation as input. However, SPMC consists of multiple MPC runs utilizing an MCS-based PV model for each run. Then, the SMPC algorithm dispatches the EVs and BSS based on the median of BSS power decisions of all runs.

Simulation results show that the SMPC algorithm can result in lower energy costs compared to the MPC algorithm. Thanks to the multiple scenario cases in the SMPC algorithm, the effects of erroneous forecasts are minimized. For further improvement, a stochastic approach can be developed for EVs, in which the EVs' entrance and leave times can be replaced with the entrance time and duration of stay in the microgrid. With this method, entrance and leave times can be coupled, giving a more realistic scenario.

For future works can be considered as:

- Cyber security and bad data identification approaches can be added to confront the possible data manipulation because of device malfunctioning or communication failure.

- Load and generation forecasts can be utilized by core-level functions to have a more efficient load management strategy.

- Reinforcement learning techniques can be used to update adjustable parameters such as K_c and K_d,

- a stochastic approach can be developed to model the EV-driver behaviors.

- Electricity market participation can be considered as a higher-level function as the monopoly systems are faded day by day.

REFERENCES

[1] U.S.-Canada Power System Outage Task Force, "Final Report on the August 14, 2003 Blackout in the United States and Canada: Causes and Recommendations," *System*, vol. 40, no. April, p. 238, 2004.

[2] J. E. Chadwick, "How a smarter grid could have prevented the 2003 U.S. cascading blackout," *2013 IEEE Power and Energy Conference at Illinois, PECI 2013*, pp. 65–71, 2013.

[3] H. L. Willis and L. Philipson, *Understanding electric utilities and de-regulation*, vol. 27. CRC Press, 2018.

[4] X. Fang, S. Misra, G. Xue, and D. Yang, "Smart grid—the new and improved power grid: A survey," *IEEE Communications Surveys & Tutorials*, vol. 14, no. 4, pp. 944–980, 2011.

[5] P. Asmus, "Microgrids, Virtual Power Plants and Our Distributed Energy Future," *The Electricity Journal*, vol. 23, pp. 72–82, dec 2010.

[6] H. Farhangi, "The path of the smart grid," *IEEE Power and Energy Magazine*, vol. 8, no. 1, pp. 18–28, 2010.

[7] M. Smith and D. Ton, "Key connections: The us department of energy: microgrid initiative," *IEEE Power and Energy Magazine*, vol. 11, no. 4, pp. 22–27, 2013.

[8] C. Marnay, G. Joos, R. Iravani, P. Mancarella, and S. Chatzivasileiadis, *Microgrids 1: Engineering, Economics, and Experience.* No. October, 2015.

[9] "2030.7-2017 - IEEE Standard for the Specification of Microgrid Controllers," *IEEE Power and Energy Society*, 2017.

[10] J. Rocabert, A. Luna, F. Blaabjerg, and P. Rodríguez, "Control of power converters in AC microgrids," *IEEE Transactions on Power Electronics*, vol. 27, no. 11, pp. 4734–4749, 2012.

[11] R. Lasseter, “MicroGrids,” *2002 IEEE Power Engineering Society Winter Meeting. Conference Proceedings (Cat. No.02CH37309)*, vol. 1, pp. 305–308, 2002.

[12] F. Katiraei, M. R. Iravani, and P. W. Lehn, “Micro-grid autonomous operation during and subsequent to islanding process,” *IEEE Transactions on Power Delivery*, vol. 20, no. 1, pp. 248–257, 2005.

[13] J. Vasiljevska and J. P. Lopes, “On the micro-grid and multi micro-grid impact assessment: Cost and benefits evaluation.,” 2011.

[14] Y. Zoka, A. Sugimoto, N. Yorino, K. Kawahara, and J. Kubokawa, “An economic evaluation for an autonomous independent network of distributed energy resources,” *Electric Power Systems Research*, vol. 77, no. 7, pp. 831–838, 2007.

[15] N. D. Hatziargyriou, A. G. Anastasiadis, J. Vasiljevska, and A. G. Tsikalakis, “Quantification of economic, environmental and operational benefits of microgrids,” in *2009 IEEE Bucharest PowerTech*, pp. 1–8, 2009.

[16] C. Marnay, J. Lai, M. Stadler, and A. Siddiqui, “Added value of reliability to a microgrid: Simulations of three california buildings,” in *2009 CIGRE/IEEE PES Joint Symposium Integration of Wide-Scale Renewable Resources Into the Power Delivery System*, pp. 1–8, 2009.

[17] P. M. Costa and M. A. Matos, “Assessing the contribution of microgrids to the reliability of distribution networks,” *Electric Power Systems Research*, vol. 79, no. 2, pp. 382–389, 2009.

[18] D. Ton and J. Reilly, “Microgrid controller initiatives,” *IEEE Power and Energy Magazine*, vol. 15, no. 4, pp. 24–31, 2017.

[19] M. Carpintero-Rentería, D. Santos-Martín, and J. M. Guerrero, “Microgrids Literature Review through a Layers Structure,” *Energies*, vol. 12, p. 4381, nov 2019.

[20] IEEE Std 1547-2008 (R2008), “IEEE Standard for interconnecting distributed resources with electric power systems amendment,” *IEEE Standards*, vol. 2014, pp. 1–16, 2008.

[21] D. G. Photovoltaics and E. Storage, "Ieee standard for interconnection and interoperability of distributed energy resources with associated electric power systems interfaces," *IEEE Std*, pp. 1547–2018, 2018.

[22] "Ieee standard for the testing of microgrid controllers," *IEEE Std 2030.8-2018*, pp. 1–42, 2018.

[23] Iec, *TECHNICAL SPECIFICATION Microgrids-Part 1: Guidelines for microgrid projects planning and specification INTERNATIONAL ELECTROTECHNICAL COMMISSION*. 2017.

[24] Iec, *TECHNICAL SPECIFICATION Microgrids-Part 1: Guidelines for microgrid projects planning and specification INTERNATIONAL ELECTROTECHNICAL COMMISSION*. 2017.

[25] P. Basak, S. Chowdhury, S. Chowdhury, and S. H. nee Dey, "Inverter based microgrid modeling & simulation," *International Journal of Distributed Energy Resources (IJDER), Germany*, pp. 1–17, 2012.

[26] F. Katiraei, R. Iravani, N. Hatziargyriou, and A. Dimeas, "Microgrid Management," *IEEE power & energy magazine*, vol. 6, no. june, pp. 54–65, 2008.

[27] H. Karimi, H. Nikkhajoei, and R. Iravani, "Control of an electronically-coupled distributed resource unit subsequent to an islanding event," *IEEE Transactions on Power Delivery*, vol. 23, no. 1, pp. 493–501, 2008.

[28] A. Bidram and A. Davoudi, "Hierarchical structure of microgrids control system," *IEEE Transactions on Smart Grid*, vol. 3, no. 4, pp. 1963–1976, 2012.

[29] a. Nasiri, "Digital Control of Three-Phase Series-Parallel Uninterruptible Power Supply Systems," *IEEE Transactions on Power Electronics*, vol. 22, no. 4, pp. 1116–1127, 2007.

[30] D. E. Olivares, A. Mehrizi-Sani, A. H. Etemadi, C. A. Cañizares, R. Iravani, M. Kazerani, A. H. Hajimiragha, O. Gomis-Bellmunt, M. Saeedifard, R. Palma-Behnke, G. A. Jiménez-Estévez, and N. D. Hatziargyriou, "Trends in microgrid control," *IEEE Transactions on Smart Grid*, vol. 5, no. 4, pp. 1905–1919, 2014.

[31] M. B. Delghavi and A. Yazdani, “An adaptive feedforward compensation for stability enhancement in droop-controlled inverter-based microgrids,” *IEEE Transactions on Power Delivery*, vol. 26, no. 3, pp. 1764–1773, 2011.

[32] R. Majumder, B. Chaudhuri, A. Ghosh, R. Majumder, G. Ledwich, and F. Zare, “Improvement of stability and load sharing in an autonomous microgrid using supplementary droop control loop,” *IEEE Transactions on Power Systems*, vol. 25, no. 2, pp. 796–808, 2010.

[33] J. A. Lopes, C. L. Moreira, and A. G. Madureira, “Defining control strategies for microgrids islanded operation,” *IEEE Transactions on Power Systems*, vol. 21, no. 2, pp. 916–924, 2006.

[34] J. Rocabert, A. Luna, F. Blaabjerg, and I. Paper, “Control of Power Converters in AC Microgrids.pdf,” *IEEE Transactions on Power Electronics*, vol. 27, no. 11, pp. 4734–4749, 2012.

[35] I.-Y. Chung and S.-J. O. Cheol-HeeYoo, “Distributed intelligent microgrid control using multi-agent systems,” *Engineering*, vol. 5, no. 1, pp. 1–6, 2013.

[36] R. Lasseter, A. Akhil, C. Marnay, J. Stephens, J. Dagle, R. Guttromsom, A. S. Meliopoulous, R. Yinger, and J. Eto, “Integration of distributed energy resources. the certs microgrid concept,” tech. rep., Lawrence Berkeley National Lab.(LBNL), Berkeley, CA (United States), 2002.

[37] R. Bayindir, E. Hossain, E. Kabalci, and R. Perez, “A comprehensive study on microgrid technology,” *International Journal of Renewable Energy Research (IJRER)*, vol. 4, no. 4, pp. 1094–1107, 2014.

[38] A. A. Zaidi and F. Kupzog, “Microgrid automation-a self-configuring approach,” in *2008 IEEE International Multitopic Conference*, pp. 565–570, IEEE, 2008.

[39] C. M. Rangel, D. Mascarella, and G. Joos, “Real-time implementation & evaluation of grid-connected microgrid energy management systems,” in *2016 IEEE Electrical Power and Energy Conference (EPEC)*, pp. 1–6, IEEE, 2016.

[40] S. Manson, B. Nayak, and W. Allen, "Robust microgrid control system for seamless transition between grid-tied and island operating modes," in *44th Annual Western Protective Relay Conference*, 2017.

[41] A. M. Ameen, J. Pasupuleti, and T. Khatib, "Simplified performance models of photovoltaic/diesel generator/battery system considering typical control strategies," *Energy Conversion and Management*, vol. 99, pp. 313–325, jul 2015.

[42] C. Sun, J. N. Paquin, F. Al Jajeh, G. Joos, and F. Bouffard, "Implementation and CHIL Testing of a Microgrid Control System," *2018 IEEE Energy Conversion Congress and Exposition, ECCE 2018*, pp. 2073–2080, dec 2020.

[43] M. A. Hannan, M. Faisal, P. Jern Ker, R. A. Begum, Z. Y. Dong, and C. Zhang, "Review of optimal methods and algorithms for sizing energy storage systems to achieve decarbonization in microgrid applications," oct 2020.

[44] C. Sun, G. Joos, S. Q. Ali, J. N. Paquin, C. M. Rangel, F. A. Jajeh, I. Novickij, and F. Bouffard, "Design and Real-Time Implementation of a Centralized Microgrid Control System with Rule-Based Dispatch and Seamless Transition Function," *IEEE Transactions on Industry Applications*, vol. 56, no. 3, pp. 3168–3177, 2020.

[45] B. Otomega, A. Marinakis, M. Glavic, and T. Van Cutsem, "Model predictive control to alleviate thermal overloads," *IEEE Transactions on Power Systems*, vol. 22, no. 3, pp. 1384–1385, 2007.

[46] A. Parisio, E. Rikos, and L. Glielmo, "A Model Predictive Control Approach to Microgrid Operation Optimization," *IEEE Transactions on Control Systems Technology*, vol. 22, no. 5, pp. 1813–1827, 2014.

[47] F. Garcia-torres and C. Bordons, "Optimal Economical Schedule of Hydrogen-Based Microgrids With Hybrid Storage Using Model Predictive Control," *IEEE Transactions on Industrial Electronics*, vol. 62, no. 8, pp. 5195–5207, 2015.

[48] A. Parisio, E. Rikos, and L. Glielmo, "Stochastic model predictive control for economic/environmental operation management of microgrids: An experimental case study," *Journal of Process Control*, vol. 43, pp. 24–37, 7 2016.

[49] M. Pereira, D. Munoz De La Pena, and D. Limon, "Robust economic model predictive control of a community micro-grid," *2016 IEEE 55th Conference on Decision and Control, CDC 2016*, vol. 100, pp. 2739–2744, 2016.

[50] B. Zhao, X. Zhang, J. Chen, C. Wang, and L. Guo, "Operation optimization of standalone microgrids considering lifetime characteristics of battery energy storage system," *IEEE Transactions on Sustainable Energy*, vol. 4, no. 4, pp. 934–943, 2013.

[51] U. Can Yilmaz, M. E. Sezgin, and M. Gol, "A Model Predictive Control for Microgrids Considering Battery Aging," *JOURNAL OF MODERN POWER SYSTEMS AND CLEAN ENERGY*, vol. 8, no. 2, 2020.

[52] Y. Li, L. Li, C. Peng, and J. Zou, "An mpc based optimized control approach for ev-based voltage regulation in distribution grid," *Electric Power Systems Research*, vol. 172, pp. 152–160, 2019.

[53] S. Wen, W. Xiong, J. Cao, and J. Qiu, "Mpc-based frequency control strategy with a dynamic energy interaction scheme for the grid-connected microgrid system," *Journal of the Franklin Institute*, vol. 357, no. 5, pp. 2736–2751, 2020.

[54] J. Pahasa and I. Ngamroo, "Simultaneous control of frequency fluctuation and battery soc in a smart grid using lfc and ev controllers based on optimal mimo-mpc," *Journal of Electrical Engineering and Technology*, vol. 12, no. 2, pp. 601–611, 2017.

[55] P. R. D. C. Mendes, J. E. Normey-Rico, and C. B. Alba, "Economic energy management of a microgrid including electric vehicles," in *2015 IEEE PES Innovative Smart Grid Technologies Latin America (ISGT LATAM)*, pp. 869–874, IEEE, 2015.

[56] T. A. N. Heirung, J. A. Paulson, J. O'Leary, and A. Mesbah, "Stochastic model predictive control—how does it work?," *Computers & Chemical Engineering*, vol. 114, pp. 158–170, 2018.

[57] M. Summerfield, *Python in Practice: Create Better Programs Using Concurrency, Libraries, and Patterns*. Addison-Wesley, 2013.

[58] C. Hunt, “1. Overview of TCP/IP - TCP/IP Network Administration, 3rd Edition [Book].”

[59] A. Paquette, R. Harley, V. Bhavaraju, S. Krstic, and P. Theisen, “Design of the fort sill microgrid,” in *2014 IEEE Energy Conversion Congress and Exposition (ECCE)*, pp. 4640–4646, IEEE, 2014.

[60] I. J. Balaguer, Q. Lei, S. Yang, U. Supatti, and F. Z. Peng, “Control for grid-connected and intentional islanding operations of distributed power generation,” *IEEE Transactions on Industrial Electronics*, vol. 58, no. 1, pp. 147–157, 2011.

[61] G. Fedele, C. Picardi, and D. Sgrò, “A power electrical signal tracking strategy based on the modulating functions method,” *IEEE Transactions on Industrial Electronics*, vol. 56, no. 10, pp. 4079–4087, 2009.

[62] A. Mellit, A. Massi Pavan, E. Ogliari, S. Leva, and V. Lughi, “Advanced methods for photovoltaic output power forecasting: A review,” *Applied Sciences*, vol. 10, no. 2, p. 487, 2020.

[63] M. Abdel-Nasser and K. Mahmoud, “Accurate photovoltaic power forecasting models using deep lstm-rnn,” *Neural Computing and Applications*, vol. 31, no. 7, pp. 2727–2740, 2019.

[64] S. Hochreiter, “Ja1 4 rgen schmidhuber (1997).“long short-term memory”,” *Neural Computation*, vol. 9, no. 8, 1997.

[65] W. F. Holmgren, R. W. Andrews, A. T. Lorenzo, and J. S. Stein, “Pvlib python 2015,” in *2015 IEEE 42nd Photovoltaic Specialist Conference (PVSC)*, pp. 1–5, 2015.

[66] M. U. Gudelek, C. R. Cirak, E. Arin, M. E. Sezgin, A. M. Ozbayoglu, and M. Gol, “Load and PV Generation Forecast Based Cost Optimization for Nanogrids with PV and Battery,” *2018 53rd International Universities Power Engineering Conference (UPEC)*, pp. 1–6, 2018.

[67] M. Prandini, S. Garatti, and J. Lygeros, “A randomized approach to stochastic model predictive control,” in *2012 IEEE 51st IEEE Conference on Decision and Control (CDC)*, pp. 7315–7320, 2012.

APPENDIX A

TABS OF THE GRAPHICAL USER INTERFACE

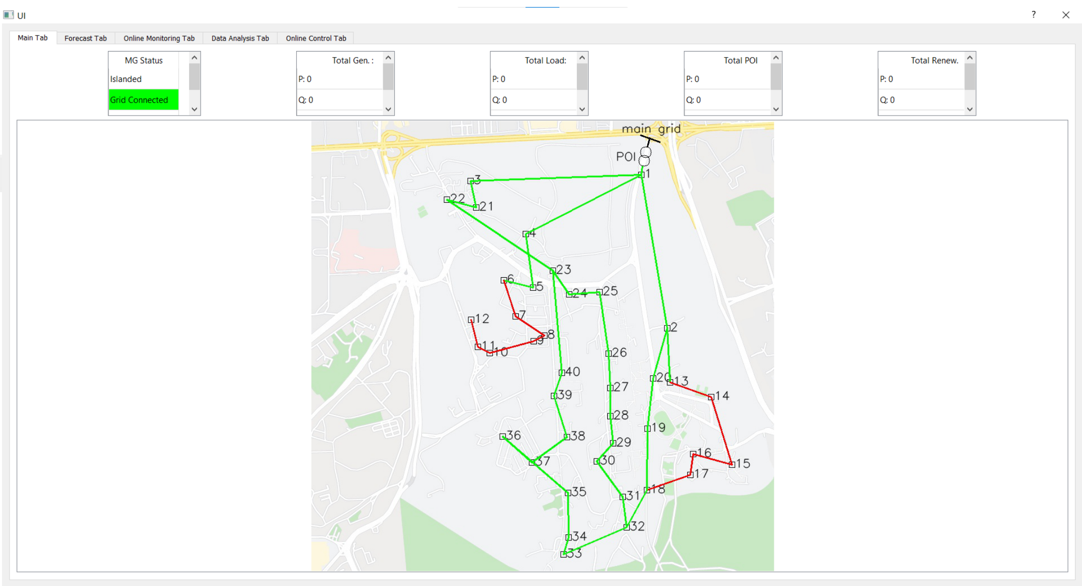

Figure A.1: Main tab

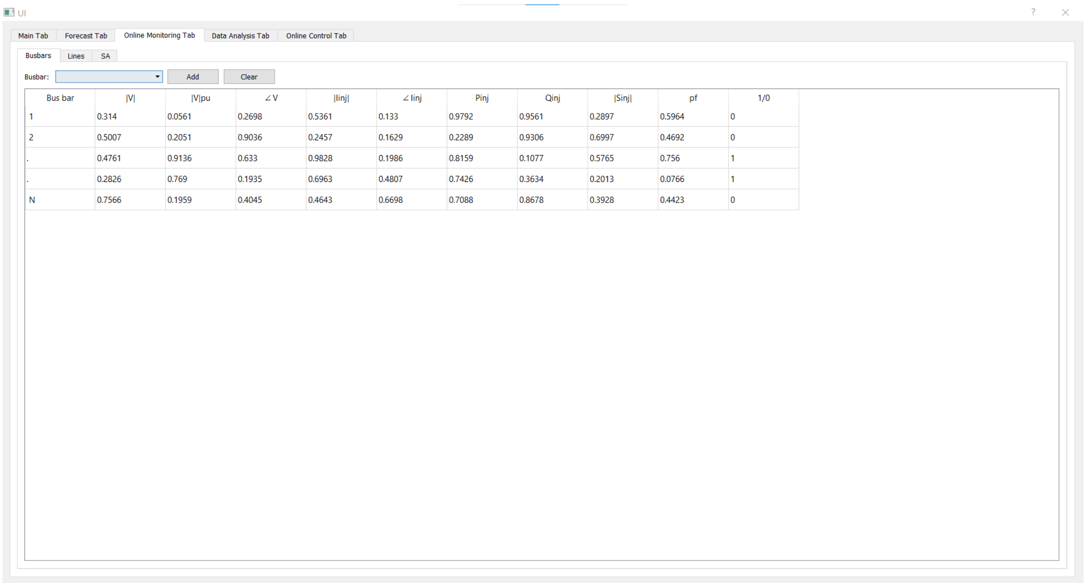

Bus bar	|V|	|V|pu	∠V	|Iinj|	∠Iinj	Pinj	Qinj	|Sinj|	pf	1/0
1	0.314	0.0561	0.2698	0.5361	0.133	0.9792	0.9561	0.2897	0.5964	0
2	0.5007	0.2051	0.9036	0.2457	0.1629	0.2289	0.9306	0.6997	0.4692	0
.	0.4761	0.9136	0.633	0.9828	0.1986	0.8159	0.1077	0.5765	0.756	1
.	0.2826	0.769	0.1935	0.6963	0.4807	0.7426	0.3634	0.2013	0.0766	1
N	0.7566	0.1959	0.4045	0.4643	0.6698	0.7088	0.8678	0.3928	0.4423	0

Figure A.2: Online monitoring tab/bus-bar

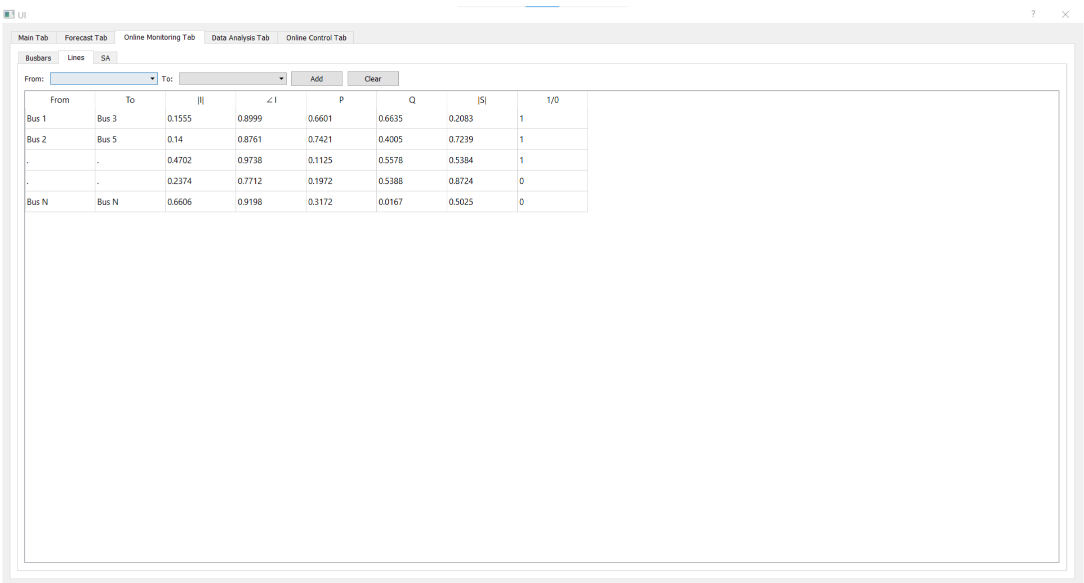

From	To	|I|	∠I	P	Q	|S|	1/0
Bus 1	Bus 3	0.1555	0.8999	0.6601	0.6635	0.2083	1
Bus 2	Bus 5	0.14	0.8761	0.7421	0.4005	0.7239	1
.	.	0.4702	0.9738	0.1125	0.5578	0.5384	1
.	.	0.2374	0.7712	0.1972	0.5388	0.8724	0
Bus N	Bus N	0.6606	0.9198	0.3172	0.0167	0.5025	0

Figure A.3: Online monitoring tab/lines

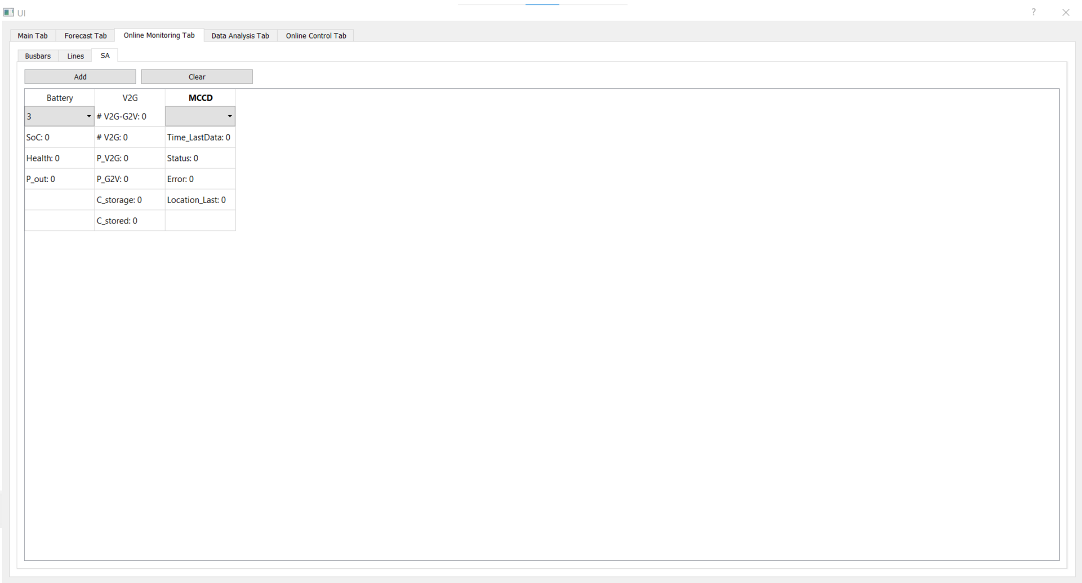

Figure A.4: Online monitoring tab/SA

Figure A.5: Forecast tab

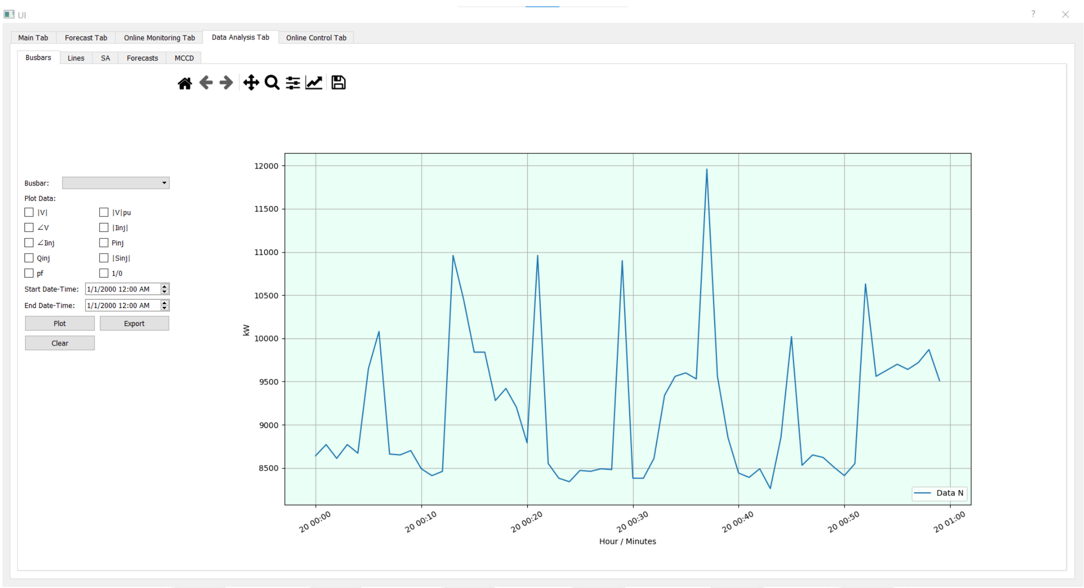

Figure A.6: Data analysis tab/bus-bar

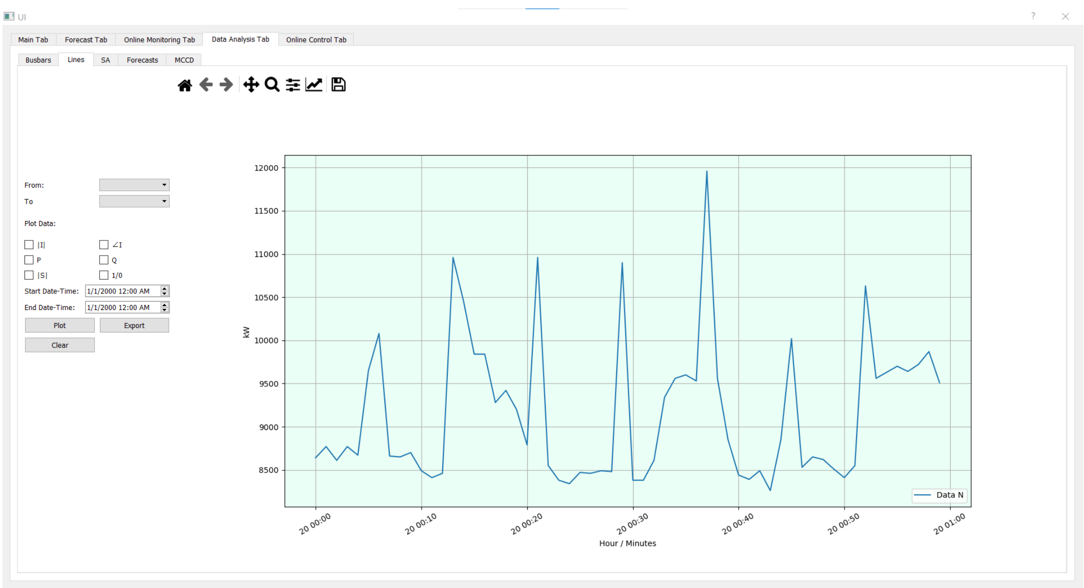

Figure A.7: Data analysis tab/lines

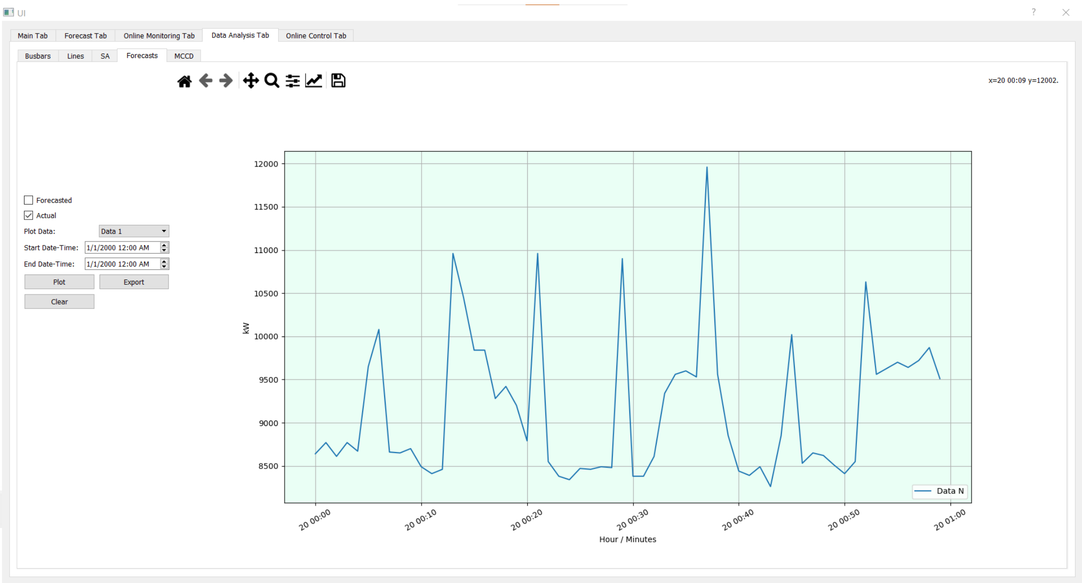

Figure A.8: Data analysis tab/forecast

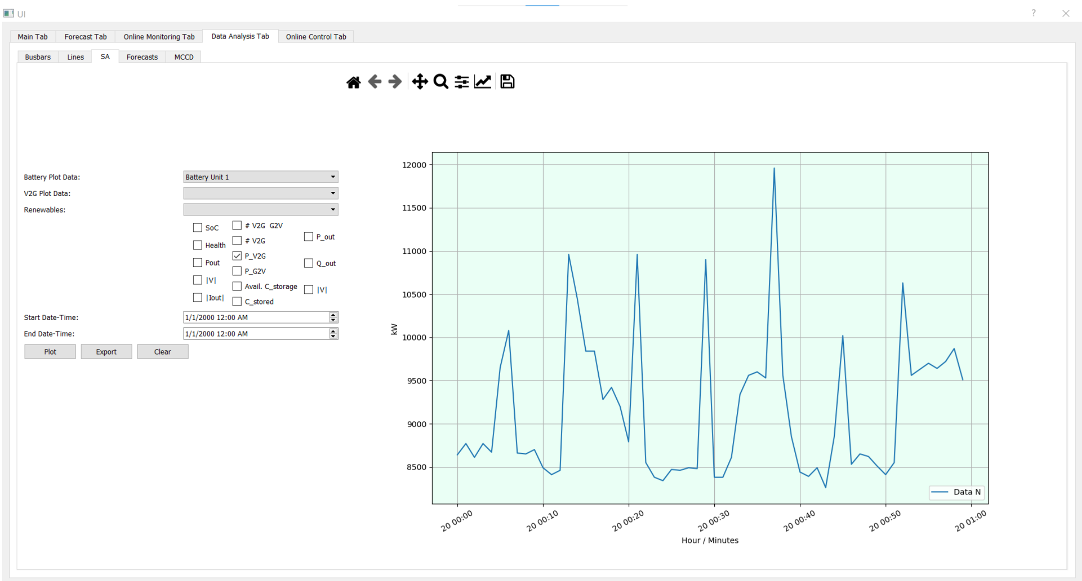

Figure A.9: Data analysis tab/smart assets

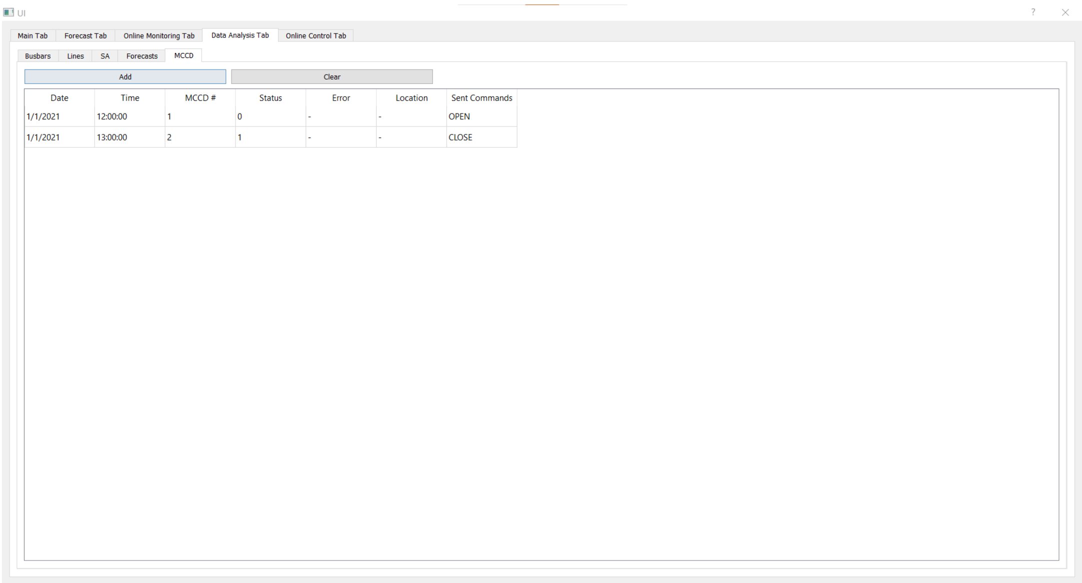

Figure A.10: Data analysis tab/MCCD

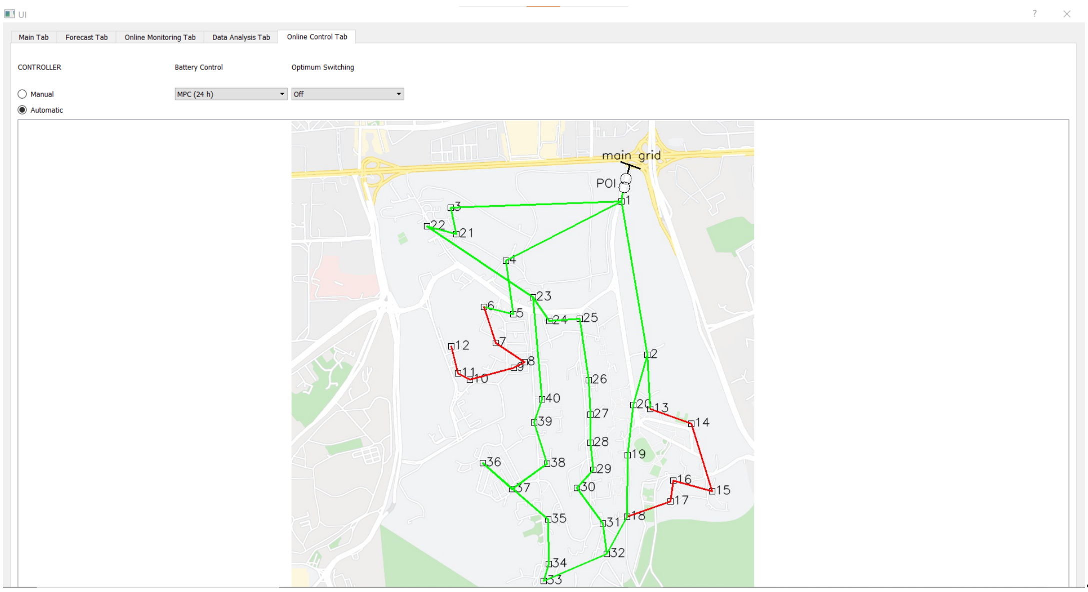

Figure A.11: Online control tab